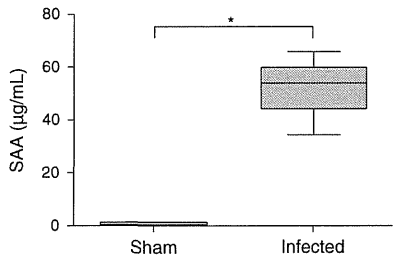

Fig. 1. Effects of oral infection with *P. gingivalis* on serum levels of serum amyloid A (SAA). All experiments were performed in triplicate wells. Significant differences were observed between the *P. gingivalis*-infected group and the sham-infected group ($n = 5$; $^*p < 0.01$, Mann–Whitney *U*-test).

insulin-like growth factor binding protein 2 (IGFBP-2) and thymus CK-1 (hereafter designated as CXCL7) were the molecules that were significantly upregulated, whereas IL-17, tumor necrosis factor α (TNF-α) and L-selectin were significantly downregulated in the infected mice (Table 2).

The levels of soluble ICAM-1 (sICAM-1) were elevated in the sera of *P. gingivalis*-infected B6.Apoeshl mice. This finding is consistent with the findings in patients with coronary artery disease (13) and implies endothelial cell, smooth-muscle cell and monocyte activation. Elevated levels of sICAM-1 may be involved in the acceleration of atherosclerotic lesion development.

CXCL7, the most abundant platelet chemokine (14), was also elevated in the infected mice. A proteolytic product of CXCL7 called neutrophil activating peptide 2 has been demonstrated to bind to chemokine (C-X-C motif) receptor (CXCR) 1 and CXCR2 (15) and to induce neutrophil adhesion to human umbilical vein endothelial cells in a dose-dependent manner *in vitro* (16). Although there is little direct evidence of a proatherogenic role for CXCL7, it is conceivable that periodontal infection is important for creating an inflammatory environment by inducing CXCL7 expression.

IGFBP-2 has been shown to play a protective role against the development of insulin resistance and obesity (17). As inflammation can promote insulin resistance and dysregulate glycemia, periodontal disease is supposed to induce insulin resistance. Although the adverse effects of periodontitis on glycemic control have not been proved, our previous study demonstrated that adiponectin receptor 2 (AdipoR2), a specific receptor for adiponectin, was downregulated in the livers of infected mice (4). This finding is of particular interest because the targeted disruption of AdipoR2 resulted in decreased activity of the peroxisome proliferator-activated receptor γ signaling pathway and in insulin resistance (18). Therefore, it is likely that IGFBP-2 is elevated to promote insulin resistance.

MMP-3 plays a pivotal role in extracellular matrix degradation in periodontal tissue during periodontopathic bacteria-induced pathogenesis. In addition, it is reported that plasma MMP-3 levels are an independent prognostic factor in coronary artery disease (19).

In contrast, plasma concentrations of TNF-α have been positively correlated with elevated plasma triglycerides and heart failure (20). In addition, TNF-α is indirectly involved in coronary heart disease risk through an increase in insulin resistance. In this respect, the downregulation of TNF-α in the infected mice compared with sham-infected mice seems to contradict the finding described above. While plasma TNF-α levels are increased in periodontitis patients compared with periodontally healthy subjects (21), these levels are increased after periodontal therapy (22). In contrast, we demonstrated that serum TNF-α levels of periodontitis patients were lower than those of control subjects. The levels were increased after successful periodontal treatment (23,24). Therefore, the downregulation of TNF-α in infected mice is consistent with the findings seen in human periodontitis patients.

Interleukin-17 plays an important pathological role in periodontal disease. Increased levels of IL-17 mRNA and protein are reported in the gingival tissue and gingival crevicular fluid of periodontitis patients (25–31). Levels of IL-17 are increased in the sera of aggressive periodontitis (32) but not of chronic periodontitis patients (33). However, the role of IL-17 in atherosclerosis remains controversial, with different studies suggesting either a proatherogenic or an atheroprotective role (34–37). Unlike human periodontitis patients, in the B6.Apoeshl mice oral infection with *P. gingivalis* downregulated the serum IL-17 levels. We are the first to demonstrate infection-induced systemic levels of IL-17 in the context of periodontal disease in mice. Although the underlying mechanisms for this downregulation are not known, given that IL-17 is protective against *P. gingivalis*-induced bone loss in a murine model (38), *P. gingivalis* oral infection may impair defense systems in hyperlipidemic conditions.

L-Selectin is a leukocyte antigen that appears to be responsible for the initial attachment of leukocytes to the endothelium and that is rapidly shed from neutrophils after chemotactic stimulation. Unlike acute inflammatory illness, patients with chronic inflammatory diseases have been shown to have lower than normal levels (39). Consistent with this finding, it is reported that patients with ischemic heart disease have lower serum soluble L-selectin (sL-selectin) levels than healthy subjects (13). Furthermore, low levels of sL-selectin have been observed in plasma from periodontitis patients (40). Decreased sL-selectin levels may reflect the sequestration of sL-selectin by widespread binding to activated endothelium.

Collectively, the present study clearly demonstrated that oral infection with *P. gingivalis* induces alteration of systemic cytokine levels, which plays a role not only in periodontal tissue destruction but also in atherogenesis in B6.Apoeshl mice. These data further support the evidence that periodontitis is associated with systemic diseases.

Acknowledgements

The authors thank Dr Yoshibumi Matsushima for kind instruction on the use of C57BL/6.KOR -*Apoe^{shl}* mice. This study was supported by the Japan Society for the Promotion of Science (23390476 and 23659974 for K.Y., 20295426 for K.T. and 21390555 for T.N., and the Young Researcher

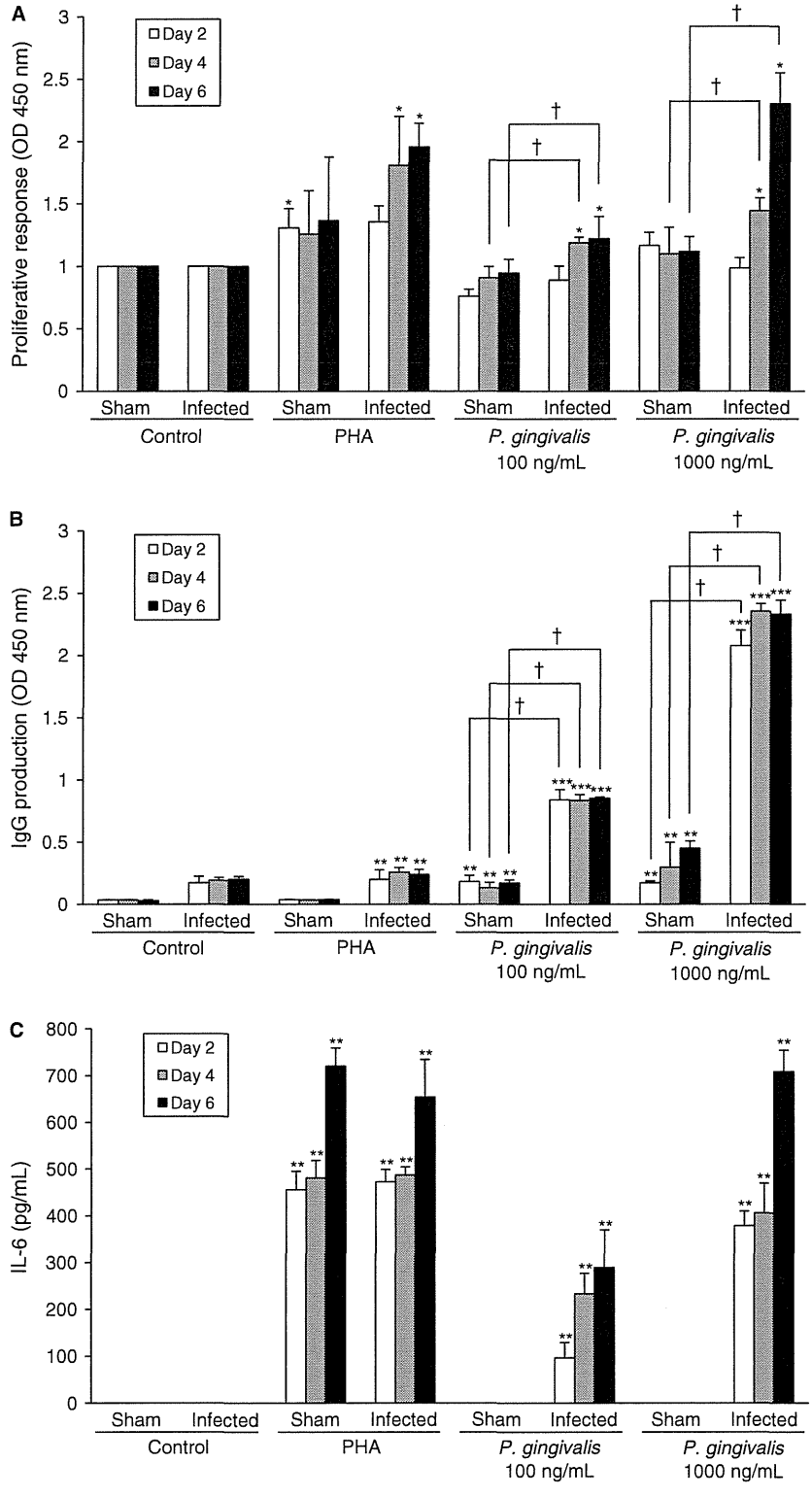

Fig. 2. Spleen cell response to *P. gingivalis* antigen. Spleen cells were stimulated with *P. gingivalis* antigen. The proliferative response (A), production of immunoglobulin G (IgG; B) and production of IL-6 (C) were compared between the sham-infected group and the *P. gingivalis*-infected group. The results are expressed as the means + SD of three mice per group. Differences in the effects of the control, phytohemagglutinin (PHA) and *P. gingivalis* antigen were analysed by Student's paired *t*-test (*$p < 0.05$; **$p < 0.01$; ***$p < 0.001$). Differences between the sham-infected and *P. gingivalis*-infected animals were analysed by Student's unpaired *t*-test (†$p < 0.05$).

Table 2. Relative cytokine levels in the sera of infected mice

Cytokine	Average fluorescence intensity		Ratio (b/a)	*p*-Value
	Sham-infected[(a)]	Infected[(b)]		
IL-17	7802.53	6094.29	0.78	0.012
L-Selectin	31498.42	23658.68	0.75	0.041
TNF-α	3265.67	2595.45	0.79	0.029
ICAM-1	977.17	1537.91	1.57	0.048
IGFBP-2	1739.88	2271.92	1.31	0.032
MMP-3	10425.64	17316.68	1.66	0.019
Thymus CK-1 (CXCL7)	24463.87	29526.76	1.21	0.009

Overseas Visits Program for Vitalizing Brain Circulation, S2203) and the Promotion of Niigata University Research Project.

References

1. Pizzo G, Guiglia R, Lo Russo L, Campisi G. Dentistry and internal medicine: from the focal infection theory to the periodontal medicine concept. *Eur J Intern Med* 2010;**21:**496–502.
2. Epstein SE, Zhou YF, Zhu J. Infection and atherosclerosis: emerging mechanistic paradigms. *Circulation* 1999;**100:**e20–e28.
3. Kiechl S, Egger G, Mayr M *et al.* Chronic infections and the risk of carotid atherosclerosis: prospective results from a large population study. *Circulation* 2001;**103:** 1064–1070.
4. Maekawa T, Takahashi N, Tabeta K *et al.* Chronic oral infection with *Porphyromonas gingivalis* accelerates atheroma formation by shifting the lipid profile. *PLoS ONE* 2011;**6:**e20240.
5. Hayashi C, Viereck J, Hua N *et al. Porphyromonas gingivalis* accelerates inflammatory atherosclerosis in the innominate artery of ApoE deficient mice. *Atherosclerosis* 2011;**215:**52–59.
6. Lalla E, Lamster IB, Hofmann MA *et al.* Oral infection with a periodontal pathogen accelerates early atherosclerosis in apolipoprotein E-null mice. *Arterioscler Thromb Vasc Biol* 2003;**23:**1405–1411.
7. Gibson FC III, Hong C, Chou HH *et al.* Innate immune recognition of invasive bacteria accelerates atherosclerosis in apolipoprotein E-deficient mice. *Circulation* 2004;**109:**2801–2806.
8. Zhang T, Kurita-Ochiai T, Hashizume T, Du Y, Oguchi S, Yamamoto M. *Aggregatibacter actinomycetemcomitans* accelerates atherosclerosis with an increase in atherogenic factors in spontaneously hyperlipidemic mice. *FEMS Immunol Med Microbiol* 2010;**59:**143–151.
9. Oh HS, Moharita A, Potian JG *et al.* Bone marrow stroma influences transforming growth factor-β production in breast cancer cells to regulate c-myc activation of the preprotachykinin-I gene in breast cancer cells. *Cancer Res* 2004; **64:**6327–6336.
10. Matsushima Y, Hayashi S, Tachibana M. Spontaneously hyperlipidemic (SHL) mice: Japanese wild mice with apolipoprotein E deficiency. *Mamm Genome* 1999;**10:**352–357.
11. Matsushima Y, Sakurai T, Ohoka A *et al.* Four strains of spontaneously hyperlipidemic (SHL) mice: phenotypic distinctions determined by genetic backgrounds. *J Atheroscler Thromb* 2001;**8:**71–79.
12. Baker PJ, Evans RT, Roopenian DC. Oral infection with *Porphyromonas gingivalis* and induced alveolar bone loss in immunocompetent and severe combined immunodeficient mice. *Arch Oral Biol* 1994;**39:** 1035–1040.
13. Haught WH, Mansour M, Rothlein R *et al.* Alterations in circulating intercellular adhesion molecule-1 and L-selectin: further evidence for chronic inflammation in ischemic heart disease. *Am Heart J* 1996;**132:**1–8.
14. Brandt E, Petersen F, Ludwig A, Ehlert JE, Bock L, Flad HD. The β-thromboglobulins and platelet factor 4: blood platelet-derived CXC chemokines with divergent roles in early neutrophil regulation. *J Leukoc Biol* 2000;**67:**471–478.
15. Gear AR, Camerini D. Platelet chemokines and chemokine receptors: linking hemostasis, inflammation, and host defense. *Microcirculation* 2003;**10:**335–350.
16. Schenk BI, Petersen F, Flad HD, Brandt E. Platelet-derived chemokines CXC chemokine ligand (CXCL)7, connective tissue-activating peptide III, and CXCL4 differentially affect and cross-regulate neutrophil adhesion and transendothelial migration. *J Immunol* 2002;**169:**2602–2610.
17. Wheatcroft SB, Kearney MT, Shah AM *et al.* IGF-binding protein-2 protects against the development of obesity and insulin resistance. *Diabetes* 2007;**56:**285–294.
18. Yamauchi T, Nio Y, Maki T *et al.* Targeted disruption of AdipoR1 and AdipoR2 causes abrogation of adiponectin binding and metabolic actions. *Nat Med* 2007;**13:**332–339.
19. Wu TC, Leu HB, Lin WT, Lin CP, Lin SJ, Chen JW. Plasma matrix metalloproteinase-3 level is an independent prognostic factor in stable coronary artery disease. *Eur J Clin Invest* 2005;**35:**537–545.
20. Jovinge S, Hamsten A, Tornvall P *et al.* Evidence for a role of tumor necrosis factor α in disturbances of triglyceride and glucose metabolism predisposing to coronary heart disease. *Metabolism* 1998;**47:** 113–118.
21. Ramirez-Tortosa MC, Quiles JL, Battino M *et al.* Periodontitis is associated with altered plasma fatty acids and cardiovascular risk markers. *Nutr Metab Cardiovasc Dis* 2010;**20:**133–139.
22. Behle JH, Sedaghatfar MH, Demmer RT *et al.* Heterogeneity of systemic inflammatory responses to periodontal therapy. *J Clin Periodontol* 2009;**36:**287–294.
23. Nakajima T, Honda T, Domon H *et al.* Periodontitis-associated up-regulation of systemic inflammatory mediator level may increase the risk of coronary heart disease. *J Periodont Res* 2010;**45:**116–122.
24. Yamazaki K, Honda T, Oda T *et al.* Effect of periodontal treatment on the C-reactive protein and proinflammatory cytokine levels in Japanese periodontitis patients. *J Periodont Res* 2005;**40:**53–58.
25. Cardoso CR, Garlet GP, Crippa GE *et al.* Evidence of the presence of T helper type 17 cells in chronic lesions of human periodontal disease. *Oral Microbiol Immunol* 2009;**24:**1–6.
26. Honda T, Aoki Y, Takahashi N *et al.* Elevated expression of IL-17 and IL-12 genes in chronic inflammatory periodontal disease. *Clin Chim Acta* 2008;**395:**137–141.
27. Johnson RB, Wood N, Serio FG. Interleukin-11 and IL-17 and the pathogenesis of periodontal disease. *J Periodontol* 2004;**75:**37–43.
28. Lester SR, Bain JL, Johnson RB, Serio FG. Gingival concentrations of interleukin-23 and -17 at healthy sites and at sites of clinical attachment loss. *J Periodontol* 2007;**78:**1545–1550.
29. Ohyama H, Kato-Kogoe N, Kuhara A *et al.* The involvement of IL-23 and the Th17 pathway in periodontitis. *J Dent Res* 2009;**88:**633–638.
30. Takahashi K, Azuma T, Motohira H, Kinane DF, Kitetsu S. The potential role of interleukin-17 in the immunopathology of periodontal disease. *J Clin Periodontol* 2005;**32:**369–374.
31. Vernal R, Dutzan N, Chaparro A, Puente J, Antonieta Valenzuela M, Gamonal J. Levels of interleukin-17 in gingival crevicular fluid and in supernatants of cellular cultures of gingival tissue from patients with chronic periodontitis. *J Clin Periodontol* 2005;**32:**383–389.
32. Schenkein HA, Koertge TE, Brooks CN, Sabatini R, Purkall DE, Tew JG. IL-17 in

sera from patients with aggressive periodontitis. *J Dent Res* 2010;**89:**943–947.
33. Özçaka Ö, Nalbantsoy A, Buduneli N. Interleukin-17 and interleukin-18 levels in saliva and plasma of patients with chronic periodontitis. *J Periodont Res* 2011;**46:** 592–598.
34. Erbel C, Chen L, Bea F *et al.* Inhibition of IL-17A attenuates atherosclerotic lesion development in apoE-deficient mice. *J Immunol* 2009;**183:**8167–8175.
35. Smith E, Prasad KM, Butcher M *et al.* Blockade of interleukin-17A results in reduced atherosclerosis in apolipoprotein E-deficient mice. *Circulation* 2010;**121:** 1746–1755.
36. Taleb S, Romain M, Ramkhelawon B *et al.* Loss of SOCS3 expression in T cells reveals a regulatory role for interleukin-17 in atherosclerosis. *J Exp Med* 2009;**206:** 2067–2077.
37. van Es T, van Puijvelde GH, Ramos OH *et al.* Attenuated atherosclerosis upon IL-17R signaling disruption in LDLr deficient mice. *Biochem Biophys Res Commun* 2009;**388:**261–265.
38. Yu JJ, Ruddy MJ, Wong GC *et al.* An essential role for IL-17 in preventing pathogen-initiated bone destruction: recruitment of neutrophils to inflamed bone requires IL-17 receptor-dependent signals. *Blood* 2007;**109:**3794–3802.
39. Spertini O, Schleiffenbaum B, White-Owen C, Ruiz P Jr, Tedder TF. ELISA for quantitation of L-selectin shed from leukocytes in vivo. *J Immunol Methods* 1992;**156:**115–123.
40. Gainet J, Dang PM, Chollet-Martin S *et al.* Neutrophil dysfunctions, IL-8, and soluble L-selectin plasma levels in rapidly progressive versus adult and localized juvenile periodontitis: variations according to disease severity and microbial flora. *J Immunol* 1999;**163:**5013–5019.

Miyazawa *et al. Lipids in Health and Disease* 2012, **11**:121
http://www.lipidworld.com/content/11/1/121

LIPIDS IN HEALTH AND DISEASE

RESEARCH Open Access

Effect of *Porphyromonas gingivalis* infection on post-transcriptional regulation of the low-density lipoprotein receptor in mice

Haruna Miyazawa[1,2], Koichi Tabeta[1*], Sayuri Miyauchi[1,2], Yukari Aoki-Nonaka[1,2], Hisanori Domon[1], Tomoyuki Honda[1,2], Takako Nakajima[1,3] and Kazuhisa Yamazaki[1,2*]

Abstract

Background: Periodontal disease is suggested to increase the risk of atherothrombotic disease by inducing dyslipidemia. Recently, we demonstrated that proprotein convertase subtilisin/kexin type 9 (PCSK9), which is known to play a critical role in the regulation of circulating low-density lipoprotein (LDL) cholesterol levels, is elevated in periodontitis patients. However, the underlying mechanisms of elevation of PCSK9 in periodontitis patients are largely unknown. Here, we explored whether *Porphyromonas gingivalis,* a representative periodontopathic bacterium, -induced inflammatory response regulates serum PCSK9 and cholesterol levels using animal models.

Methods: We infected C57BL/6 mice intraperitoneally with *Porphyromonas gingivalis*, a representative strain of periodontopathic bacteria, and evaluated serum PCSK9 levels and the serum lipid profile. PCSK9 and LDL receptor (LDLR) gene and protein expression, as well as liver X receptors (*Lxrs*), inducible degrader of the LDLR (*Idol*), and sterol regulatory element binding transcription factor (*Srebf)2* gene expression, were examined in the liver.

Results: *P. gingivalis* infection induced a significant elevation of serum PCSK9 levels and a concomitant elevation of total and LDL cholesterol compared with sham-infected mice. The LDL cholesterol levels were significantly correlated with PCSK9 levels. Expression of the *Pcsk9*, *Ldlr*, and *Srebf2* genes was upregulated in the livers of the *P. gingivalis*-infected mice compared with the sham-infected mice. Although *Pcsk9* gene expression is known to be positively regulated by sterol regulatory element binding protein (SREBP)2 (human homologue of Srebf2), whereas *Srebf2* is negatively regulated by cholesterol, the elevated expression of *Srebf2* found in the infected mice is thought to be mediated by *P. gingivalis* infection.

Conclusions: *P. gingivalis* infection upregulates PCSK9 production via upregulation of *Srebf2*, independent of cholesterol levels. Further studies are required to elucidate how infection regulates *Srebf2* expression and subsequently influences lipid metabolism.

Keywords: PCSK9, LDL cholesterol, Periodontitis, Chronic inflammation

* Correspondence: koichi@dent.niigata-u.ac.jp; kaz@dent.niigata-u.ac.jp
[1]Center for Transdisciplinary Research, Niigata University, 5274 Gakkocho 2-ban-cho, Chu-o-ku, Niigata 951-8514, Japan
[2]Laboratory of Periodontology and Immunology, Division of Oral Science for Health Promotion, Niigata University Graduate School of Medical and Dental Sciences, 5274 Gakkocho 2-ban-cho, Chu-o-ku, Niigata 951-8514, Japan
Full list of author information is available at the end of the article

Background

Periodontitis is associated with atherosclerotic vascular disease, as it induces dyslipidemia. It has been found that periodontitis decreases HDL cholesterol and increases LDL cholesterol levels. It has also been reported that the presence of periodontal pockets was positively associated with higher LDL and total cholesterol in humans [1]. Löesche *et al.* showed that the levels of total and LDL cholesterol were significantly higher in 50- to 60-year-old patients with moderate periodontitis compared with age- and sex-matched controls [2]. Furthermore, intensive periodontal therapy consisting of subgingival mechanical debridement with adjunctive local delivery of minocycline significantly decreased total and LDL cholesterol compared with baseline levels [3]. The mechanisms underlying the elevation of LDL cholesterol levels in periodontitis patients have not yet been elucidated.

Plasma cholesterol levels are regulated by the LDL receptor (LDLR). The number of LDLRs expressed on the hepatocyte surface is the primary determinant of plasma cholesterol levels and is therefore strictly regulated. Transcription of the LDLR gene is controlled by cellular cholesterol levels through the sterol regulatory element-binding protein (SREBP) [4] and Liver X receptors (LXRs) [5]. Additionally, post-transcriptional regulation of LDLR expression is a major determinant of lipoprotein metabolism.

Proprotein convertase subtilisin/kexin type 9 (PCSK9) post-transcriptionally promotes the degradation of LDLRs in hepatocytes [6]. PCSK9 is mainly expressed in the liver, intestine, and kidney, and it is secreted into the plasma [7]. This protein does not directly degrade LDLRs but binds to LDLRs at epidermal growth factor-like repeats. This binding decreases LDLR recycling to the cell surface and promotes lysosomal degradation [8], which results in decreased numbers of LDLRs and increased plasma LDL levels. We have recently shown that serum levels of PCSK9 are significantly increased in periodontitis patients compared with periodontally healthy subjects [9]. In addition to PCSK9, the inducible degrader of the LDL receptor (Idol) has been shown to play an important role in the post-transcriptional regulation of LDLRs. Zelcer *et al.* [5] found that LDLR expression is controlled by the LXR-Idol axis as LXR induces Idol, which is an E3 ubiquitin ligase that triggers LDLR degradation.

It is well-recognized that infection and inflammation induce marked changes in lipid and lipoprotein metabolism [10]. However, there is little information about the effects of infection on PCSK9 or Idol levels and subsequent expression of LDLR and cholesterol levels. Only one study has shown that inflammatory stimuli, such as lipopolysaccharide or zymosan, markedly increased hepatic PCSK9 mRNA expression, resulting in decreased LDLR protein expression [11]. Therefore, in the present study, we analyzed the effects of infection with *Porphyromonas gingivalis*, a representative strain of periodontopathic bacteria, on the regulation of PCSK9 and subsequently expression of LDLR in the liver.

Results

Serum SAA and PCSK9 levels

Systemic infection with *P. gingivalis* induced a significant elevation of serum amyloid A (SAA) levels. The PCSK9 levels in the infected mice were significantly higher than in the sham-infected mice (Figure 1).

Plasma lipid profiles

The total and LDL cholesterol levels were significantly higher in the *P. gingivalis*-infected mice compared with the sham-infected mice. In contrast, HDL cholesterol levels tended to be lower in the *P. gingivalis*-infected mice than the sham-infected mice. There was no difference in triglyceride levels between the *P. gingivalis*-infected mice and sham-infected mice (Figure 2).

Relationship between serum PCSK9 and LDL cholesterol levels

Similar to a previous study by our group that demonstrated a close relationship between PCSK9 and LDL cholesterol, we found a significant correlation between PCSK9 levels and LDL cholesterol levels after *P. gingivalis* infection (Figure 3).

However, no correlations were observed between PCSK9 levels and total cholesterol levels, HDL cholesterol levels, or triglyceride levels (data not shown).

PCSK9 and LDLR gene and protein expression in the liver

There was a significant increase in the expression of PCSK9 and LDLR (Figure 4A) in the infected mice compared to the sham-infected mice. However, there was a much larger increase in gene expression observed for PCSK9 than LDLR. Although *Pcsk9* gene expression was increased, the levels of mature PCSK9 protein in the liver of the *P. gingivalis*-infected mice were similar to those of the sham-infected mice. Pro-PCSK9 protein levels were even lower in the *P. gingivalis*-infected mice compared with the sham-infected mice. In contrast to the gene expression results, the protein levels of LDLR were significantly lower in the livers of the *P. gingivalis*-infected mice compared with the sham-infected mice (Figure 4B and C).

Changes in *Srebf2*, *Lxrs*, and *Idol* gene expression

SREBP2 (Srebf2 in mice) is a major activator of PCSK9 signaling. Therefore, the effect of *P. gingivalis* infection on PCSK9 expression was analyzed. As shown in Figure 5A, *Srebf2* expression was significantly upregulated in the

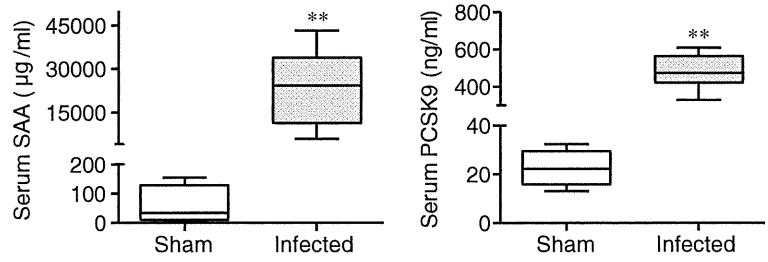

Figure 1 Effects of *P. gingivalis* infection on serum levels of serum amyloid A (SAA) and PCSK9 (N = 5 in the sham-infected group; N = 6 in the infected group). All samples were analyzed in duplicate for each condition. Box plots represent medians, with the 25th and 75th percentiles shown as boxes and the 10th and 90th percentiles as whiskers. Significant differences were observed between the infected group and the sham-infected group (** $P < 0.01$, Mann–Whitney U-test).

P. gingivalis-infected mice compared with the sham-infected mice.

Because of the important role of Idol in the post-transcriptional regulation of LDLR expression, the effects of *P. gingivalis* infection on *Idol* gene expression and the gene expression of *Lxrs*, a regulator of the *Idol* gene, were examined. *Idol* gene expression was slightly, but significantly suppressed in the *P. gingivalis*-infected mice compared with the sham-infected mice (Figure 5B). However, no differences in *Lxrα* or *Lxrβ* gene expression were observed, although the expression of both genes tended to be higher in the *P. gingivalis*-infected mice (Figure 5C).

Discussion

Given that humans with loss-of-function mutations in the *PCSK9* gene [12] and mice lacking *Pcsk9* expression exhibit significantly reduced circulating LDL cholesterol levels [13], whereas activating mutations in the *PCSK9* gene result in severe familial hypercholesterolemia [14] accompanied by increased cardiovascular risk, PCSK9 is considered at present to be an important therapeutic target for combating hypercholesterolemia [15]. In addition, other factors that elevate circulating PCSK9 levels could be considered to be risk factors for coronary heart disease (CHD). A previous study by our group demonstrated that periodontitis, a chronic inflammatory disease induced by a group of periodontopathic bacteria, could elevate serum PCSK9 levels [9]. However, the underlying mechanisms by which periodontal infection affects PCSK9 levels and the subsequent alterations of the plasma lipid profile are not known.

It is well-known that infection and inflammation induce an acute phase response, which leads to multiple alterations in lipid and lipoprotein metabolism [10]. We have

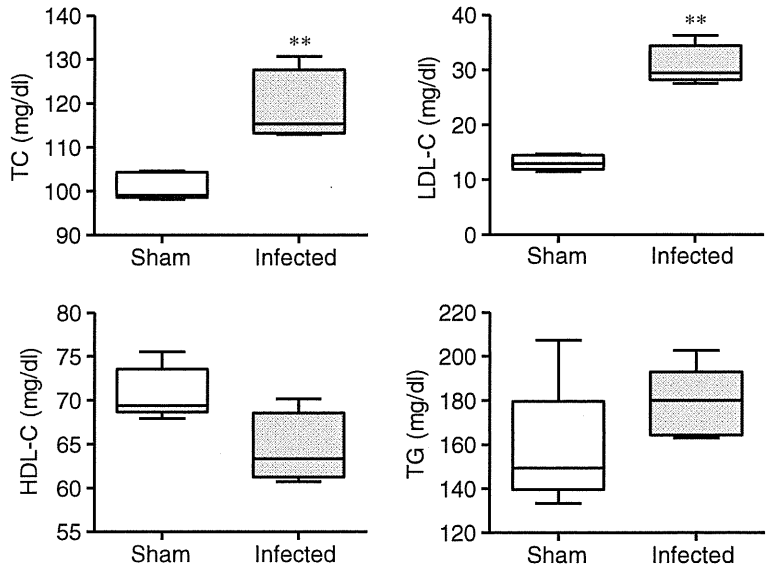

Figure 2 Effects of *P. gingivalis* infection on the plasma lipid profile (N = 5 in each group). Box plots represent medians, with the 25th and 75th percentiles as boxes and the 10th and 90th percentiles as whiskers. Total and LDL cholesterol levels were significantly higher, whereas HDL cholesterol levels tended to be lower in the *P. gingivalis*-infected mice (** $P < 0.01$, Mann–Whitney U-test).

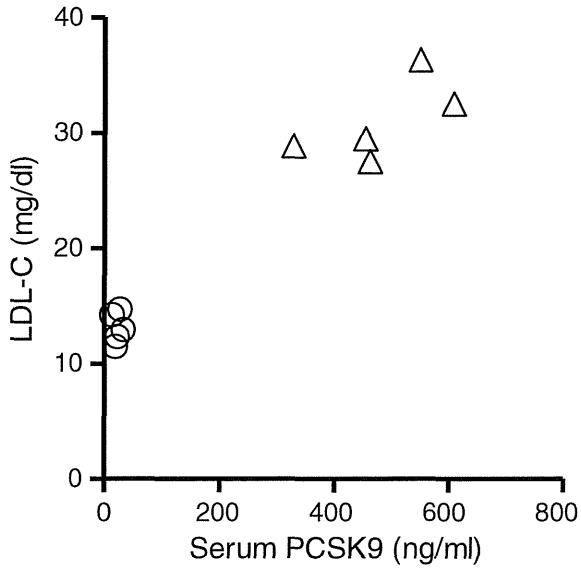

Figure 3 Relationship between serum PCSK9 and LDL cholesterol levels in the *P. gingivalis*-infected (open triangle) and sham-infected (open circle) mice (N = 5 in each group). Spearman's rank correlation coefficient analysis showed that there was a significant correlation between LDL cholesterol levels and serum PCSK9 levels. Spearman r = 0.8545, $P < 0.01$.

shown that chronic oral infection with *P. gingivalis* induced downregulation of HDL cholesterol by suppressing Liver X receptors and their target gene *Abca1* in C57BL/6 mice and ApoE-deficient C57BL/6.KOR-*Apoe*^{shl} (B6.Apoeshl) mice [16]. Furthermore, as in human periodontitis patients, the LDL cholesterol levels were elevated in *P. gingivalis*-infected B6.Apoeshl mice. However, the molecular basis for the elevation of LDL cholesterol was not analyzed in this experimental setting.

This study is the first to show that infection induces a significant increase in circulating PCSK9 levels and a concomitant decrease of LDLR levels in mice. Furthermore, there was a significant correlation found between LDLR gene expression in the liver and the serum levels of PCSK9. In this study, infection was induced via intraperitoneal, rather than oral, bacterial inoculation. Although oral infection can mimic human periodontal disease, and it is clear that oral infection with *P. gingivalis* does, in fact, affect *Pcsk9* gene expression in the liver (data not shown), subsequent change in lipid metabolism can be easily observed in peritoneal infection model.

Pcsk9 gene expression was significantly upregulated in the liver of the *P. gingivalis*-infected mice. Previous studies have demonstrated that *Pcsk9* and *Ldlr* gene transcription is regulated by sterol regulatory element-binding proteins (SREBPs) [17,18]. Consistent with these studies, *Srebf2* expression was found to be significantly upregulated in the livers of the *P. gingivalis*-infected mice compared with the sham-infected mice. *Srebf2* expression is downregulated by cholesterol and upregulated by statin treatment. As total and LDL cholesterol were elevated in the *P. gingivalis*-infected mice, *Srebf2* is likely to be induced by this infection. Although the mechanisms by which infection and/or inflammation induce the upregulation of *Srebf2* are not clear, our study suggests that additional mechanisms related to infection induce hyperlipidemia during infection.

Recently, another transcription factor, known as hepatocyte nuclear factor-1α (HNF1α), was reported to be involved in the transcriptional regulation of the *Pcsk9* gene in mammalian HepG2 cells [19]. However, it has not been reported whether *Pcsk9* is activated by HNF1α in mice. Therefore, other mechanisms may regulate *Pcsk9* expression during infection; further studies will be needed to answer this question.

In contrast to the gene expression results, the level of mature PCSK9 protein in the liver was unchanged in the *P. gingivalis*-infected mice compared to the sham-infected mice, whereas the levels of PCSK9 proprotein were slightly reduced in the *P. gingivalis*-infected mice. Because we failed to observe the enhanced transcription of PCSK9 in other organ specimen such as liver, kidney, jejulium, ilenium, aolta, and spleen (data not shown), we speculate that secreted PCSK9 immediately infiltrate into circulation and result in the elevation of PCSK9 levels higher in the *P. gingivalis*-infected mice. Recently, it has become evident that domain interactions are important for the regulation of PCSK9 protein secretion [20]. However, it remains to be elucidated how infection affects PCSK9 protein secretion.

Similar to *Pcsk9*, *Ldlr* is upregulated in the livers of the *P. gingivalis*-infected mice compared with the sham-infected mice, although to a much lesser degree. Because LDLR expression is also positively regulated by SREBP2 [18], upregulation of *Ldlr* could be an effect of the infection. Contrary to what was observed regarding *Ldlr* gene expression, LDLR protein expression in the liver of the *P. gingivalis*-infected mice was significantly reduced compared with the sham-infected mice. Although the *Ldlr* gene expression levels in the *P. gingivalis*-infected mice were 2 times higher compared with the sham-infected mice, the expression of LDLR protein was decreased, possibly because PCSK9 serum levels were increased more than 20 fold in the infected mice.

In addition to PCSK9, LDLR expression is controlled by the LXR-Idol axis, in which LXR induces Idol, an E3 ubiquitin ligase that triggers LDLR degradation [5]. The importance of Idol in the regulation of LDLR expression is increasingly being recognized [21]. Therefore, the affect of *P. gingivalis* infection on *Idol* gene expression was analyzed. Although the expression of the *Idol* gene was significantly down-regulated in the *P. gingivalis*-infected mice, the difference in *Idol* gene expression between the

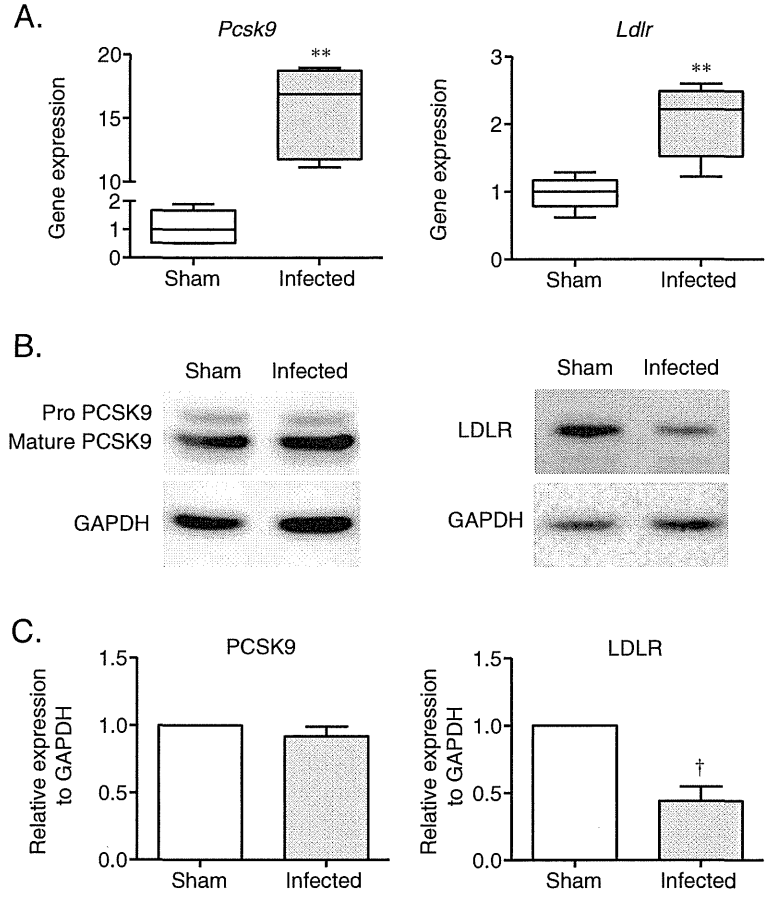

Figure 4 Effect of *P. gingivalis* infection on PCSK9 and LDLR gene and protein expression in the liver. Total RNA and protein were extracted from the *P. gingivalis*-infected and sham-infected mice, and the samples were analyzed by quantitative RT-PCR or western blotting. *Pcsk9* and *Ldlr* gene expression was significantly higher in the *P. gingivalis*-infected mice compared with the sham-infected mice (** $P < 0.01$, Mann–Whitney U-test). The PCSK9 protein levels of were unchanged in the *P. gingivalis*-infected mice compared with the sham-infected mice. LDLR protein levels were significantly lower in the *P. gingivalis*-infected mice compared with the sham-infected mice († $P < 0.05$, unpaired t-test).

infected and the sham-infected mice was smaller than what was observed for *Pcsk9*. In addition, the expression of *Lxrs* did not differ between the *P. gingivalis*-infected mice and the sham-infected mice. Therefore, it is possible that *P. gingivalis* infection does not affect LDLR expression by downregulating *Idol* in this experimental model.

Our study supports the previously described notion that bacterial infections alter the plasma lipid profile based on the novel finding that *P. gingivalis* infection elevates PCSK9 expression in the liver by increasing *Srebf2* expression through a currently unidentified mechanism. The effects of infection and inflammation on lipid and lipoprotein metabolism are complex, and contrasting results are often demonstrated between rodents and primates [10]. Our animal study model has potential limitations considering the characteristics of chronic inflammation in human periodontitis, because peritoneal infection in mice induces robust acute immune response. There may be other proteins that are involved in the regulation of PCSK9 by the mechanisms related to inflammation. Further studies will be required to gain insight into the role of PCSK9 in the dyslipidemia that accompanies infections and chronic inflammatory diseases, such as periodontitis.

Conclusions

We found that *P. gingivalis* infection upregulates PCSK9 production via upregulation of *Srebf2*, independent of cholesterol levels resulting elevation of LDL cholesterol. Further studies are required to elucidate how infection regulates *Srebf2* expression and subsequently influences lipid metabolism.

Methods

Mice

All experiments were performed in accordance with the Regulations and Guidelines on Scientific and Ethical Care and Use of Laboratory Animals of the Science Council of Japan, enforced on June 1, 2006 and approved

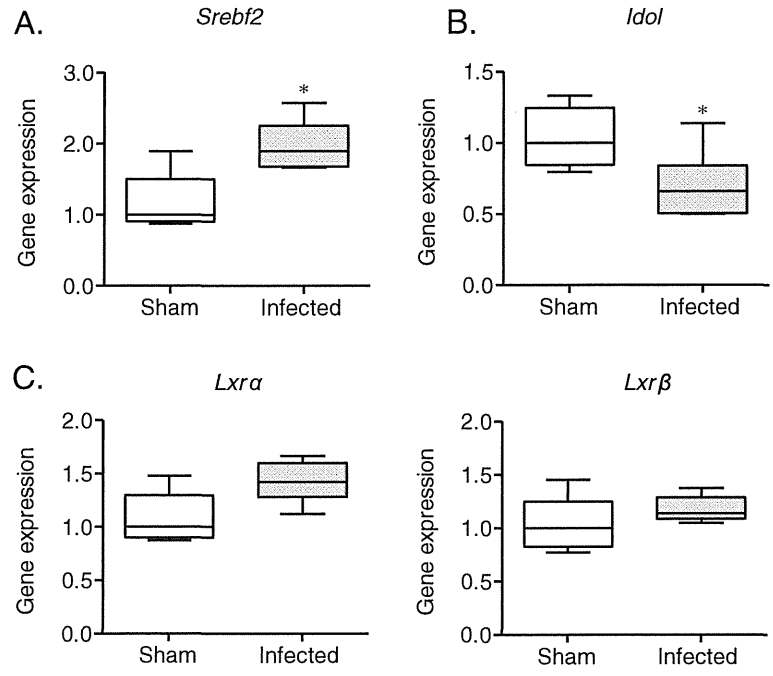

Figure 5 Comparison of the relative gene expression levels in the liver between the *P. gingivalis*-infected mice and the sham-infected mice (N = 5 in the sham-infected group, N = 6 in the infected group). The relative mRNA levels for the investigated genes were normalized to the relative glyceraldehyde-3-phosphate dehydrogenase (GAPDH) mRNA levels. The box plots represent medians, with the 25th and 75th percentiles being depicted as boxes and the 10th and 90th percentiles presented as whiskers. Significant differences were observed for *Srebf2* and *Idol* (* $P < 0.05$, Mann–Whitney U-test).

by the Institutional Animal Care and Use Committee at Niigata University (permit number 231–1). Six-week-old male C57BL/6 mice were obtained from Japan SLC, Inc. (Shizuoka, Japan). The mice were maintained under pathogen-free conditions and were fed regular chow and sterile water until they were infected.

Bacterial cultures and infection

P. gingivalis strain W83 was cultured in modified Gifu anaerobic medium (GAM) broth (Nissui, Tokyo, Japan) in an anaerobic jar (Becton Dickinson Microbiology Systems, Cockeysville, MD) in the presence of an AnaeroPack™ (Mitsubishi Gas Chemical Co. Inc., Tokyo, Japan) for 48 hours at 37°C. Bacterial suspensions were prepared in Mg^{2+}/Ca^{2+}-free phosphate-buffered saline (PBS) using spectrophotometry to establish growth curves. The number of CFUs was standardized by measuring the optical density at 600 nm. The mice in the experimental groups were administered a single intraperitoneal (i.p.) inoculum of 10^9 CFU in 0.2 ml of sterile phosphate-buffered saline (PBS), pH 7.2. Control mice were inoculated with PBS alone. Mice were euthanized 16 hrs after infection and then analyzed.

Real-time PCR

Total RNA was isolated from the liver using TRIzol™ (Life Technologies, Carlsbad, CA) according to the manufacturer's instructions. Next, aliquots of RNA were reverse transcribed to produce cDNA using random primers (Takara Bio Inc., Shiga, Japan) and M-MLV reverse transcriptase (Life Technologies, Carlsbad, CA). Specific primers and probes for real-time PCR were purchased from Applied Biosystems (Foster City, CA). TaqMan Gene Expression Assays (Applied Biosystems) were performed in 20-μl reactions containing 900 nM primers and 250 nM probe using an ABI PRISM 7900HT Sequence Detection System (Applied Biosystems). The reaction conditions involved a 10-minute incubation at 95°C followed by 40 cycles of a two-step amplification procedure consisting of annealing/extension at 60°C for 1 minute and denaturation for 15 seconds at 95°C. ABI PRISM SDS 2.0 software (Applied Biosystems) was used to analyze the standards and quantify the data. The relative quantity of each mRNA sequence was normalized to the relative quantity of glyceraldehyde-3-phosphate dehydrogenase (GAPDH) mRNA.

Western blotting

The livers of the mice were dissected into small pieces, and protein was extracted using T-PER Tissue Protein Extraction Reagent (Thermo Scientific, Rockford, IL) supplemented with a Halt Protease Inhibitor Cocktail Kit (Thermo Scientific) and Halt Phosphatase Inhibitor

Cocktail (Thermo Scientific) according to the manufacturer's instructions. Cell debris was pelleted by centrifugation at 10,000 × *g* for 5 minutes at 4°C. The protein concentration in the supernatant was determined using the Pierce BCA Protein Assay kit (Thermo Scientific) according to the manufacturer's instructions.

Thirty micrograms of each sample were solubilized in SDS sample buffer, separated by SDS-PAGE, and transferred to a polyvinylidene difluoride membrane (Immobilon-P; Millipore Co., Bedford, MA). The samples were subsequently subjected to western blotting with rabbit anti-mouse PCSK9 (Abcam, Cambridge, UK) or rabbit anti-mouse LDLR (Abcam) primary antibodies followed by ECL™ Peroxidase labeled anti-rabbit secondary antibodies (GE Healthcare, Buckinghamshire, UK). The blots were developed with ECL using Lumi Vision PRO 400EX (Aisin, Aichi, Japan). The membranes were then washed 3 times with wash buffer (Tris-buffered saline containing 0.1% Tween-20 and 0.5% BSA) and reprobed with goat anti-mouse GAPDH antibodies (Santa Cruz Biotechnology, Santa Cruz, CA), as described above. Horseradish peroxidase-labeled donkey anti-goat IgG (Santa Cruz) was used as secondary antibody for reprobing. The intensity of the signal was quantified with Scion Image 4.02 computer software. The intensity of each protein band was normalized to the intensity of GAPDH.

Serum PCSK9, SAA, and lipoprotein levels

SAA and PCSK9 were measured using commercially available ELISA kits (Tridelta Development Ltd., Kildare, UK and R & D Systems, Minneapolis, MN, respectively) in serum collected prior to euthanasia. Serum cholesterol and triglyceride profiles were analyzed at Skylight Biotech Inc. (Akita, Japan).

Statistical analyses

The differences in the examined gene expression and biochemical parameters between the infected and control mice were analyzed using the Mann–Whitney U-test. Linear correlations were obtained using Spearman's rank correlation coefficient analysis. Unpaired t-tests were used for densitometric analysis. The statistical analyses were performed using standard statistical software (GraphPad Prism, GraphPad Software Inc., La Jolla, CA and StatView J-5.0 application program, SAS Institute Inc., Cary, NC). $P < 0.05$ was considered to be statistically significant.

Abbreviations

PCSK9: Proprotein convertase subtilisin/kexin type 9; LDL: Low-density lipoproteins; HDL: High-density lipoproteins; LDLR: LDL receptor; LXR: Liver X receptor; Idol: Inducible degrader of the LDLR; Srebf2: Sterol regulatory element binding transcription factor2; SREBP: Sterol regulatory element binding protein; LPS: Lipopolysaccharide; B6.Apoeshl: C57BL/6.KOR-*Apoe*^{shl}; HNF1α: Hepatocyte nuclear factor-1.

Competing interests

The authors declare that they have no competing interests.

Authors' contributions

KT, TN, and KY designed the study; HM, SM, YA-N, HD and TM performed the experiments; KT, TN and KY wrote the paper. All authors read and approved the final manuscript.

Acknowledgements

This study was supported by the Japan Society for the Promotion of Science (23390476 and 23659974 for KY, 20295426 for KT, and 21390555 for TN), the Young Researcher Overseas Visits Program for Vitalizing Brain Circulation (S2203), and the Promotion of Niigata University Research Project.

Author details

[1]Center for Transdisciplinary Research, Niigata University, 5274 Gakkocho 2-ban-cho, Chu-o-ku, Niigata 951-8514, Japan. [2]Laboratory of Periodontology and Immunology, Division of Oral Science for Health Promotion, Niigata University Graduate School of Medical and Dental Sciences, 5274 Gakkocho 2-ban-cho, Chu-o-ku, Niigata 951-8514, Japan. [3]General Dentistry and Clinical Education Unit, Niigata University Medical and Dental Hospital, 5274 Gakkocho 2-ban-cho, Chu-o-ku, Niigata 951-8514, Japan.

Received: 24 May 2012 Accepted: 14 September 2012
Published: 19 September 2012

References

1. Katz J, Flugelman MY, Goldberg A, Heft M: **Association between periodontal pockets and elevated cholesterol and low density lipoprotein cholesterol levels.** *J Periodontol* 2002, **73**:494–500.
2. Losche W, Karapetow F, Pohl A, Pohl C, Kocher T: **Plasma lipid and blood glucose levels in patients with destructive periodontal disease.** *J Clin Periodontol* 2000, **27**:537–541.
3. D'Aiuto F, Nibali L, Parkar M, Suvan J, Tonetti MS: **Short-term effects of intensive periodontal therapy on serum inflammatory markers and cholesterol.** *J Dent Res* 2005, **84**:269–273.
4. Yokoyama C, Wang X, Briggs MR, Admon A, Wu J, Hua X, Goldstein JL, Brown MS: **SREBP-1, a basic-helix-loop-helix-leucine zipper protein that controls transcription of the low density lipoprotein receptor gene.** *Cell* 1993, **75**:187–197.
5. Zelcer N, Hong C, Boyadjian R, Tontonoz P: **LXR regulates cholesterol uptake through Idol-dependent ubiquitination of the LDL receptor.** *Science* 2009, **325**:100–104.
6. Lambert G, Charlton F, Rye KA, Piper DE: **Molecular basis of PCSK9 function.** *Atherosclerosis* 2009, **203**:1–7.
7. Seidah NG, Benjannet S, Wickham L, Marcinkiewicz J, Jasmin SB, Stifani S, Basak A, Prat A, Chretien M: **The secretory proprotein convertase neural apoptosis-regulated convertase 1 (NARC-1): liver regeneration and neuronal differentiation.** *Proc Natl Acad Sci US A* 2003, **100**:928–933.
8. Zhang DW, Lagace TA, Garuti R, Zhao Z, McDonald M, Horton JD, Cohen JC, Hobbs HH: **Binding of proprotein convertase subtilisin/kexin type 9 to epidermal growth factor-like repeat A of low density lipoprotein receptor decreases receptor recycling and increases degradation.** *J Biol Chem* 2007, **282**:18602–18612.
9. Miyazawa H, Honda T, Miyauchi S, Domon H, Okui T, Nakajima T, Tabeta K, Yamazaki K: **Increased serum PCSK9 concentrations are associated with periodontal infection but do not correlate with LDL cholesterol concentration.** *Clin Chim Acta* 2012, **413**:154–159.
10. Khovidhunkit W, Kim MS, Memon RA, Shigenaga JK, Moser AH, Feingold KR, Grunfeld C: **Effects of infection and inflammation on lipid and lipoprotein metabolism: mechanisms and consequences to the host.** *J Lipid Res* 2004, **45**:1169–1196.
11. Feingold KR, Moser AH, Shigenaga JK, Patzek SM, Grunfeld C: **Inflammation stimulates the expression of PCSK9.** *Biochem BiophysRes Commun* 2008, **374**:341–344.
12. Cohen J, Pertsemlidis A, Kotowski IK, Graham R, Garcia CK, Hobbs HH: **Low LDL cholesterol in individuals of African descent resulting from frequent nonsense mutations in PCSK9.** *Nat Genet* 2005, **37**:161–165.
13. Rashid S, Curtis DE, Garuti R, Anderson NN, Bashmakov Y, Ho YK, Hammer RE, Moon YA, Horton JD: **Decreased plasma cholesterol and**

hypersensitivity to statins in mice lacking Pcsk9. *Proc Natl Acad Sci U S A* 2005, **102**:5374–5379.
14. Abifadel M, Varret M, Rabes JP, Allard D, Ouguerram K, Devillers M, Cruaud C, Benjannet S, Wickham L, Erlich D, *et al*: **Mutations in PCSK9 cause autosomal dominant hypercholesterolemia.** *Nat Genet* 2003, **34**:154–156.
15. Lambert G, Krempf M, Costet P: **PCSK9: a promising therapeutic target for dyslipidemias?** *Trends Endocrinol Metab* 2006, **17**:79–81.
16. Maekawa T, Takahashi N, Tabeta K, Aoki Y, Miyashita H, Miyauchi S, Miyazawa H, Nakajima T, Yamazaki K: **Chronic Oral Infection with *Porphyromonas gingivalis* accelerates atheroma formation by shifting the lipid profile.** *PLoS ONE* 2011, **6**:e20240.
17. Dubuc G, Chamberland A, Wassef H, Davignon J, Seidah NG, Bernier L, Prat A: **Statins upregulate PCSK9, the gene encoding the proprotein convertase neural apoptosis-regulated convertase-1 implicated in familial hypercholesterolemia.** *Arterioscler Thromb Vasc Biol* 2004, **24**:1454–1459.
18. Jeong HJ, Lee HS, Kim KS, Kim YK, Yoon D, Park SW: **Sterol-dependent regulation of proprotein convertase subtilisin/kexin type 9 expression by sterol-regulatory element binding protein-2.** *J Lipid Res* 2008, **49**:399–409.
19. Li H, Dong B, Park SW, Lee HS, Chen W, Liu J: **Hepatocyte nuclear factor 1alpha plays a critical role in PCSK9 gene transcription and regulation by the natural hypocholesterolemic compound berberine.** *J Biol Chem* 2009, **284**:28885–28895.
20. Du F, Hui Y, Zhang M, Linton MF, Fazio S, Fan D: **Novel domain interaction regulates secretion of proprotein convertase subtilisin/kexin type 9 (PCSK9) protein.** *J Biol Chem* 2011, **286**:43054–43061.
21. Sorrentino V, Zelcer N: **Post-transcriptional regulation of lipoprotein receptors by the E3-ubiquitin ligase inducible degrader of the low-density lipoprotein receptor.** *Curr Opin Lipidol* 2012, **23**(3):213–219.

doi:10.1186/1476-511X-11-121
Cite this article as: Miyazawa *et al.*: Effect of *Porphyromonas gingivalis* infection on post-transcriptional regulation of the low-density lipoprotein receptor in mice. *Lipids in Health and Disease* 2012 **11**:121.

THE JOURNAL OF BIOLOGICAL CHEMISTRY VOL. 287, NO. 13, pp. 10590–10601, March 23, 2012
Published in the U.S.A.

Role of Epithelial-Stem Cell Interactions during Dental Cell Differentiation*[S]

Received for publication, August 4, 2011, and in revised form, January 5, 2012 Published, JBC Papers in Press, February 1, 2012, DOI 10.1074/jbc.M111.285874

Makiko Arakaki[‡1], Masaki Ishikawa[§1], Takashi Nakamura[‡], Tsutomu Iwamoto[‡], Aya Yamada[‡], Emiko Fukumoto[‡], Masahiro Saito[¶], Keishi Otsu[‖], Hidemitsu Harada[‖], Yoshihiko Yamada[§], and Satoshi Fukumoto[‡2]

From the [‡]Division of Pediatric Dentistry, Department of Oral Health and Development Sciences, Tohoku University Graduate School of Dentistry, Sendai 980-8575, Japan, the [§]Laboratory of Cell and Developmental Biology, NIDCR, National Institutes of Health, Bethesda, Maryland 20892, the [¶]Faculty of Industrial Science and Technology, Tokyo University of Science, Chiba 278-8510, Japan, and the [‖]Department of Oral Anatomy II, Iwate Medical College School of Dentistry, Morioka 020-8505, Japan

Background: The role of dental epithelium in stem cell differentiation has not been clearly elucidated.
Results: SP cells differentiated into odontoblasts by epithelial BMP4, whereas iPS cells differentiated into ameloblasts when cultured with dental epithelium.
Conclusion: Stem cells can be induced to odontogenic cell fates when co-cultured with dental epithelium.
Significance: This is the first report to show induction of ameloblasts from iPS cells.

Epithelial-mesenchymal interactions regulate the growth and morphogenesis of ectodermal organs such as teeth. Dental pulp stem cells (DPSCs) are a part of dental mesenchyme, derived from the cranial neural crest, and differentiate into dentin forming odontoblasts. However, the interactions between DPSCs and epithelium have not been clearly elucidated. In this study, we established a mouse dental pulp stem cell line (SP) comprised of enriched side population cells that displayed a multipotent capacity to differentiate into odontogenic, osteogenic, adipogenic, and neurogenic cells. We also analyzed the interactions between SP cells and cells from the rat dental epithelial SF2 line. When cultured with SF2 cells, SP cells differentiated into odontoblasts that expressed dentin sialophosphoprotein. This differentiation was regulated by BMP2 and BMP4, and inhibited by the BMP antagonist Noggin. We also found that mouse iPS cells cultured with mitomycin C-treated SF2-24 cells displayed an epithelial cell-like morphology. Those cells expressed the epithelial cell markers p63 and cytokeratin-14, and the ameloblast markers ameloblastin and enamelin, whereas they did not express the endodermal cell marker Gata6 or mesodermal cell marker brachyury. This is the first report of differentiation of iPS cells into ameloblasts via interactions with dental epithelium. Co-culturing with dental epithelial cells appears to induce stem cell differentiation that favors an odontogenic cell fate, which may be a useful approach for tooth bioengineering strategies.

Tooth morphogenesis is characterized by reciprocal interactions between dental epithelium and mesenchymal cells derived from the cranial neural crest, which result in formation of the proper number and shapes of teeth. Multiple extracellular signaling molecules, including BMPs, FGFs, WNTs, and SHH, have been implicated in these interactions for tooth development (1). Epithelial cells then subsequently give rise to enamel-forming ameloblasts, while mesenchymal stem cells (MSCs)[3] form dentin-forming odontoblasts and dental pulp cells. Initial tooth development is also regulated by extracellular matrices (ECMs), such as basement membrane components that include laminin, collagen, fibronectin, and perlecan (2, 3). These matrices control proliferation, polarity, and attachment, and also determine tooth germ size and morphology. At later stages of tooth development, the basement membrane components disappear and odontogenic cells begin to secrete a variety of tooth-specific extracellular matrices that give rise to layers of enamel and dentin, produced by epithelial-derived ameloblasts and mesenchymal-derived odontoblasts, respectively. Ameloblastin (Ambn) is one of the enamel matrix proteins expressed by differentiating ameloblasts, and is essential for dental epithelial cell differentiation into ameloblasts and enamel formation (2, 4). Dentin sialophosphoprotein (DSPP) is a member of the SIBLING (Small Integrin-Binding Ligand *N*-linked Glycoprotein) family of extracellular matrix glycophosphoproteins, and is expressed by differentiating ameloblasts and odontoblasts (5). These extracellular matrices are important for the formation of enamel and dentin (2).

Stem cell research has identified and established several types of stem cells, including induced pluripotent stem (iPS) cells, which are generated from a variety of somatic cell types via introduction of transcription factors that mediate pluripo-

* This work was supported, in whole or in part, by the Intramural Research Program of the NIDCR, National Institutes of Health (to Y. Y.). This work was also supported by Grants-in-aid 20679006 (to S. F.), 21792054 (to A. Y.), 21792154 (to E. F.) from the Ministry of Education, Science, and Culture of Japan, and the NEXT program (LS010, to S. F.), and by grants from the Takeda Science Foundation.

[S] This article contains supplemental Figs. S1–S5 and Table S1.

[1] Both authors contributed equally to this work.

[2] To whom correspondence should be addressed: Division of Pediatric Dentistry, Department of Oral Health and Development Sciences, Tohoku University Graduate School of Dentistry, Sendai 980-8575, Japan. Fax: 81-22-717-8386; E-mail: fukumoto@dent.tohoku.ac.jp.

[3] The abbreviations used are: MSC, mesenchymal stem cell; mDP, mouse dental pulp; Ambn, Ameloblastin; DSPP, dentin sialophosphoprotein; iPS, induced pluripotent stem; DPSC, dental pulp stem cell; SP, side population; MP, majority population; ALP, alkaline phosphatase; MEF, mouse embryonic fibroblasts; MMC, mitomycin C.

tency (6). Direct reprogramming of somatic cells into iPS cells by forced expression of a small number of defined factors (*e.g.* Oct3/4, Sox2, Klf4, and c-Myc) has great potential for tissue-specific regenerative therapies. In addition, this process also avoids ethical issues surrounding the use of embryonic stem (ES) cells, as well as problems with rejection following implantation of non-autologous cells (7). A variety of cell types, including hematopoietic precursor cells (8, 9), endothelial cells, MSCs, neuronal cells (10), reproductive cells (11), and cardiomyocytes (12, 13), undergo *in vitro* differentiation. However previous studies of dental cell differentiation are not adequate to explain this process. Several dental stem cell populations have been identified in different parts of the tooth, including cells from the periodontal ligament that links the tooth root with the bone, tips of developing roots, and tissue (dental follicle) that surrounds an unerupted tooth. In addition, dental pulp stem cells (DPSCs) have been identified in the pulp of exfoliated deciduous teeth of both children and adults (14). These different cell types likely share a common lineage, being derived from neural crest cells, and all have generic MSC-like properties.

Transplantation of *in vitro* expanded DPSCs mixed with hydroxyapatite/tricalcium phosphate particles results in the formation of dental pulp and dentin-like tissue complexes in immunocompromised mice (15). Similar results have been observed with an MSC population obtained from human exfoliated deciduous teeth (SHED) (14). DPSCs also express the putative stem cell marker STRO-1 and perivascular cell marker CD146, while a proportion co-expresses smooth muscle actin and the pericyte-associated antigen 3G5 (16). These findings suggest that a population of DPSCs may reside in this perivascular niche within the pulp of adult teeth.

Side population (SP) cells were identified by flow cytometry analysis with a Hoechst 33342 efflux assay and found to have stem cell characteristics (17). SP cells are a small population that show low levels of Hoechst dye staining for the expression of Abcg2, an ATP-binding cassette transporter (18), which is strongly expressed in dental pulp in human adult and deciduous teeth (19). Dental pulp contains multipotent stem cells and is viewed as a potential source of iPS cells (14, 20, 21). In tooth germ development, undifferentiated neural crest-derived MSCs interact with dental epithelium and differentiate into dentin matrix-secreting odontoblasts. However, the interactions between stem cells and dental epithelium have not been clearly elucidated.

In this study, we established an SP cell line from mouse dental papilla. We then cultured these SP cells with rat dental epithelial cells to investigate epithelial-mesenchymal interactions. SP cells were induced to differentiate into DSPP expressing odontoblasts via the action of epithelial BMP4. Furthermore, mouse iPS cells differentiated into Ambn-expressing dental epithelium when cultured with dental epithelial cells. Thus, these undifferentiated stem cells can be induced to an odontogenic cell fate when co-cultured with dental epithelial cells. These findings may be useful for analysis of dental cell differentiation *in vitro* and for procurement of odontogenic cells for use in regenerative medicine.

EXPERIMENTAL PROCEDURES

Preparation of Mouse Dental Papilla Cells—Dental papilla tissues were isolated from incisors from newborn ICR mice by digesting with 0.1% collagenase D (Roche) and 2.5% trypsin for 30 min at 37 °C. Enzymatically digested tissues were minced into 2–4 mm pieces using micro-scissors and washed three times with Dulbecco's modified Eagle's medium (DMEM) (Invitrogen) containing 10% fetal bovine serum (FBS) (Invitrogen) and an antibiotic-antimycotic mixture (Invitrogen), then filtered through a cell strainer (40 μm) to eliminate clumps and debris. Mouse dental papilla (mDP) cells were cultured in 60-mm culture dishes and immortalized by expression of a mutant human papilloma virus type 16 E6 gene lacking the PDZ-domain-binding motif (22). mDP cells were maintained with DMEM supplemented with 10% FBS and an antibiotic-antimycotic mixture at 37 °C in a humidified atmosphere containing 5% CO_2.

Generation of Dental Epithelial Cell Line SF2-24 and Cell Culture—Rat dental epithelial cells were enzymatically isolated from the cervical loop at the apical end of the lower incisors from a Sprague-Dawley rat with 1% collagenase. Dental epithelial cells were cultured with DMEM (Invitrogen) supplemented with 10% FBS for 4 weeks, then, maintained in serum-free keratinocyte synthetic medium (Keratinocyte-SFM, Invitrogen) for 1 year. An established cell line, SF2 was maintained as previously described (4). SF2 cells were transfected with a pEF6/GFP-PDGFtm-myc-HA vector expressing the GFP-PDGF receptor-transmembrane fusion protein with myc-HA tag using Lipofectamine 2000 (Invitrogen). Transfected cells were selected as SF2 subclones by culturing with media containing 400 μg/ml of G418. Twenty-five clones were selected as a stable transfected cell line, with one of them designated as SF2-24 (Ambn high expression) and another SF2-7 (Ambn low expression).

SP and MP Cell Analysis and Flow Cytometry—Hoechst staining of mDP cells for SP cell analysis was conducted as previously described (17). Subconfluent mDP cells were stained with Hoechst dye for 90 min at 37 °C. After staining, all cells were resuspended in 100 μl of Hanks' balanced salt solution (HBSS) with calcium/magnesium medium and kept on ice. The SP and MP gates were defined as previously described (17). For analysis, the cells were resuspended in ice-cold HBSS with 2% FBS containing propidium iodide (Sigma) at a final concentration of 2 μg/ml to identify dead cells, then filtered through a cell strainer. Sorting and analyses were carried out with an EPICS ALTRA flow cytometer (Beckman Coulter, Fullerton, CA). The SP cell fraction was enriched by repeating cell sorting 3 times. The expression of stem cell markers in SP cells was confirmed by flow cytometry using anti-Sca-1 and Oct3/4 antibodies (Santa Cruz Biotechnology).

Differentiation of SP Cells—For odontoblastic induction, SP cells were plated at 6×10^4 cells in 60-mm dishes. After the cells had reached 50–60% confluence, we replaced the control medium with induction medium containing 100 ng/ml of BMP2 or BMP4 (Wako Pure Chemical Industries), and cells were incubated for 2 days. For blocking BMP signaling, recombinant mouse Noggin protein (R&D systems) was

used. Total RNA was isolated and real time RT-PCR was performed using mouse Bcrp1 (18) and DSPP primer sets (supplemental Table S1).

For adipogenic differentiation, SP cells were seeded at 1×10^5 cells per well in 6-well plates and cultured in DMEM supplemented with 10% FBS. Adipogenic differentiation was induced with induction medium from a Poietics hMSC Media Bullet kit (Cambrex Bio Science Walkersville, Inc., Walkersville, MD) for 3 days and incubated in maintenance medium for 3 days, then the cells were cultured for an additional 7 days in maintenance medium. As a control, cells were cultured in only maintenance medium. Adipogenesis was confirmed by staining with Oil-Red-O and the expression of *PPARγ* was analyzed by RT-PCR.

For osteogenic differentiation, SP cells were seeded at 1.5×10^4 cells per well in 6-well plates and cultured in DMEM supplemented with 10% FBS, 10 mM β-glycerophosphate, 0.2 mM ascorbic acid, 2-phosphate, and 10^{-8} M dexamethasone. Induction and control media were replaced every 2 days. Osteogenesis was determined by alkaline phosphatase (ALP) and von Kossa staining for calcium deposition, as previously described (23). After 4 weeks culturing with osteoblast induction medium, the expressions of osteocalcin, osteonectin, and Runx2 in osteogenesis-induced SP cells were analyzed by RT-PCR.

For neurogenic differentiation, we modified a neuronal induction protocol using recombinant nerve growth factor (NGF) (Chemicon). SP cells were seeded at 1×10^5 cells per well in 6-well plates. After reaching 80–90% confluence, neurogenic differentiation was induced by culturing the cells in DMEM supplemented 2% FBS, 1.25% dimethyl sulfoxide, 10^{-6} M retinoic acid, 2.5 μg/ml insulin, and 50 ng/ml NGF. Two weeks later, neurogenesis was characterized by Western blot analysis using an anti-neurofilament-M specific antibody (Cell Signaling Technology).

Odontoblastic Induction of SP Cells by Co-culturing with Dental Epithelial Cells—We investigated the role of dental epithelial cells in specification of odontogenic cell lineage using two types of co-culture systems: feeder and chamber types with a cell culture insert (BD Falcon). We used confluent SF2 cells, or SF2 cells treated with 4% paraformaldehyde (PFA) or ammonium (denudation) as feeder cells. SF2 and SP cells were harvested and placed into either 6-well plates or cell culture inserts (chamber), then cultured until reaching confluence.

Screening of Co-culture Conditions for Ameloblastic Induction of iPS Cells—A mouse iPS cell line (iPS-MEF-Ng-20D-17), carrying the Nanog-GFP/IRES/puromycin resistant gene, was established by Yamanaka (Kyoto University, Japan), and obtained from RIKEN Cell Bank (Saitama, Japan) (6). Mouse iPS cells were cultured with rat dental epithelial cells (SF2-24), which predominantly express Ambn mRNA, as feeder cells. Preparatory co-culture experiments were performed as follows: iPS cells were cultured with mouse embryonic fibroblasts (MEFs) treated with mitomycin C (MMC) or with three different types of SF2-24 feeder cells (confluent cells, cells treated with MMC, cells treated with 4% PFA). MMC was supplied at 9 μg/ml (final concentration) for 2 h to arrest SF2-24 cell proliferation.

Induction of iPS Cell-derived Ameloblasts—iPS cells (plated $1.5 \times 10^3/cm^2$) were cultured on sheets of MMC-treated SF2-24 cells for 7, 10, and 14 days in the same medium used for the SF2-24 culture without leukemia inhibitory factor and 2-mercaptoethanol. The culture medium was changed every day throughout the co-culture period. After 7 and 10 days, the co-cultured iPS cells were subjected to RT-PCR, while those after 14 days of culture were analyzed by immunocytochemistry. Total RNA from iPS cells co-cultured with MMC-treated MEFs was isolated after 3 days of culture. Conditioned media from cultures of SF2-24 and SF2-7 were collected after 2 days of incubation. The procedures used for transfection of Ambn-expressing vectors, as well as their construction and isolation of recombinant proteins have been previously described (2, 24). K252a (Trk inhibitor, Calbiochem), PD98059 (MEK inhibitor, Cell signaling), anti-NT-4 neutralizing antibody (Applied Biological Materials), and Noggin (R&D systems) were added to conditioned medium obtained from SF2-24 cells.

Reverse Transcription-PCR—Total RNA was isolated using TRIzol (Invitrogen) and first-strand cDNA was synthesized at 50 °C for 50 min using oligo(dT) or random primers with the SuperScript III First-strand Synthesis System (Invitrogen). PCR was performed with Takara Ex Taq HotStart Version (Takara) or a PCR Additives Kit (Jena Bioscience, Germany). The primer sequences are presented in supplemental Table S1. PCR amplicons were separated and visualized on 1.5% agarose gels with SYBR Green staining using the LAS-4000 mini image analyzing system (Fujifilm). For semi-quantitative PCR analysis, the band intensities of PCR amplicons were quantified using MultiGauge software (Fujifilm) and normalized by dividing the intensity of the band of GAPDH. Because of the high degree of homology between the Ambn gene in mice and rats (94.2%), we designed a species-specific mouse Ambn primer that encoded locked nucleic acid (LNA) at a different base sequence between the mouse and rat Ambn gene in a conserved region. The specificity of the mouse Ambn primer was confirmed by PCR using mouse and rat tooth germ cDNA. Statistical analysis of gene expression was performed using the Student's *t* test.

Immunocytochemistry—For immunocytochemistry, cells were fixed with 4% PFA for 5 min at room temperature. After washing with PBS three times for 5 min, the cells were treated with Power Block Universal Reagent (BioGenex) for 5 min at room temperature, followed by three washes with PBS. The cells were incubated with the anti-Ambn primary antibody included in the kit (1:200, M-300, Santa Cruz Biotechnology). The primary antibody was visualized with Alexa Fluor 594 donkey anti-rabbit antibody (1:500, A21207, Invitrogen). Nuclei were stained with Hoechst 33258 (Invitrogen). Immunocytochemistry and phase images were captured using a BZ-8000 microscopic system (KEYENCE Co, Osaka, Japan), and images of the sections were analyzed using a BZ analyzer (KEYENCE).

RESULTS

Establishment of SP Cell Line from Mouse Dental Papilla Cells—Side population (SP) cells, which displayed stem cell ability, make up less than 1% of total cells in the mouse dental papilla (mDP) from postnatal tooth germs. Thus, biochemical and biomolecular analyses of SP cells are difficult to perform

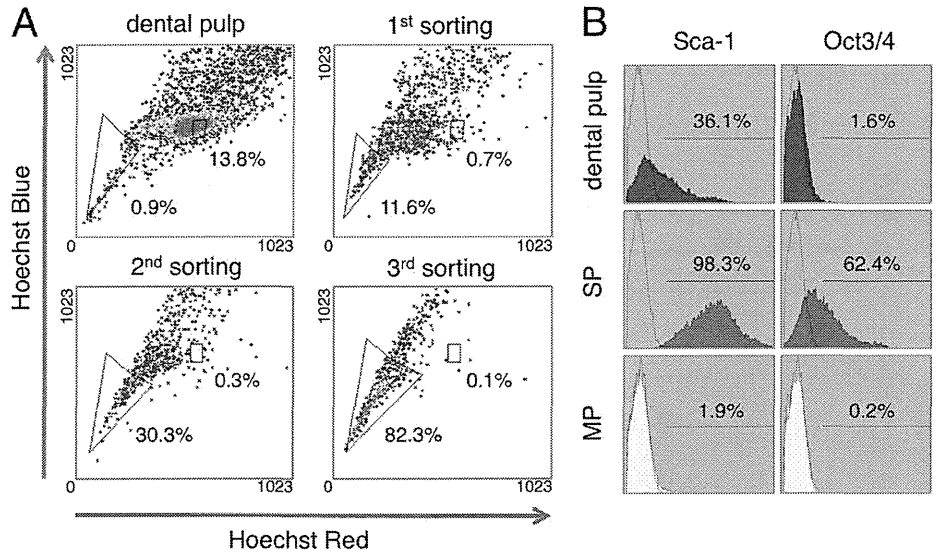

FIGURE 1. **Isolation of SP cells from mDP cell line.** *A*, flow cytometry analysis of SP cells. mDP cells made up ~0.9% of the total cell population with a relatively lower level of Hoechst 33342 fluorescence (SP cells), while 13.8% of the population was maintained as MP cells. Using repeated cell sorting, the SP cell population was enriched by 11.6% at the first sorting, 30.3% at the second sorting, and 82.3% at the third sorting. *B*, expression of the stem cell markers Sca-1 and Oct3/4 in dental pulp, SP, and MP cells.

because of the limited numbers of cells available. We enriched an SP cell population and established an SP cell line using a cell sorting technique. mDP cells were obtained from mouse incisor tooth germs and immortalized, as previously described (22). The cells were then stained with Hoechst dye and sorted to enrich the SP cell fraction. Cell sorting was repeated three times and SP cells were enriched from about 0.9% to 82.3% in the gated area (Fig. 1*A*). This SP cell line showed high expression levels of the stem cell markers Sca-1 and Oct3/4 when compared with the majority population (MP) cells, which was comprised of a greater number dental papilla cells in various differentiation stages (Fig. 1*B*).

Because the SP cells expressed a set of stem cell markers, we examined their multipotency. Using an odontoblast differentiation medium containing BMP2 or BMP4, the SP cells were induced to express DSPP, a marker of odontoblasts, whereas the expression of the undifferentiated cell marker Bcrp1 was decreased (Fig. 2*A*). In osteoblast differentiation medium, the SP cells showed increased levels of ALP and von Kossa staining, as well as expressions of the osteoblast marker genes osteocalcin, osteonectin, and Runx2, whereas the MP cells showed no induction of expression of those genes (Fig. 2, *B* and *C*). When SP cells were cultured in differentiation medium for adipogenesis or neurogenesis, they were Oil-Red-O positive or showed neurite outgrowths, along with high levels of adipogenic expression and protein expressions of neurogenic markers, such as *PPARγ* and Neurofilament-M, respectively (supplemental Fig. S1, *A--D*). These results suggest that the SP cell line established in this study has a high level of multipotency.

Expressions of Runx2 and DSPP in SP Cells Cultured with SF2 Cells—We analyzed epithelial and mesenchymal stem cell interactions by culturing SP cells with rat dental epithelial SF2 cells that had been engineered to express a GFP-myc-HA tag on the cell membrane surface. This allowed us to distinguish between SP and SF2 cell types (supplemental Fig. S2). SP cells were cultured with or without SF2 cells for 48 h, and total RNA was isolated from the mixed cell cultures (Fig. 3*A*). The expressions of Runx2 and DSPP were increased in SP cells that had been cultured with SF2 cells, as compared with those cultured without SF2 cells (Fig. 3*B*). Because Runx2 and DSPP are expressed by both odontoblasts and ameloblasts, co-cultured SP and SF2 cells were separated into individual cell populations using the anti-HA antibody, which specifically recognizes SF2 cells (Fig. 3*C*). We found a dramatic increase in the expression level of Runx2 in SF2 cells as compared with SP cells (Fig. 3*D*). No epithelial marker was detected in SP cells co-cultured with SF2 cells, suggesting that the SP cells had differentiated into odontoblasts (data not shown). Runx2 is expressed in enamel matrix-secreting ameloblasts, but not in the pre-secretion stage of ameloblasts (25). Our results suggest that the SF2 cells had fully differentiated into enamel matrix-secreting ameloblasts by co-culturing with SP cells. The expression of DSPP was up-regulated in both cell types. However, in MP cells, which are fully differentiated dental papilla cells, no expression of Runx2 or DSPP was induced by co-culturing with SF2 cells (data not shown). These results indicate that epithelial and mesenchymal stem cell interactions promote individual differential states in SF2 and SP cells.

Involvement of Exogenous Factors from Dental Epithelium in DSPP Expression of SP Cells—We attempted to identify the factors in dental epithelial cells involved in SP cell differentiation by treating SF2 cells with 4% PFA to inhibit extracellular signaling, including the effects of growth factors (Fig. 4*A*). Ammonia treatment, through a process known as denudation, removes all cell components except the extracellular matrices and is often used for three-dimensional matrix cell culture experiments (26). DSPP expression in SP cells was partially inhibited by PFA treatment, while they retained the extracellular matrix network. This result suggests that the extracellular environment including extracellular matrices, growth factors, and cell-cell

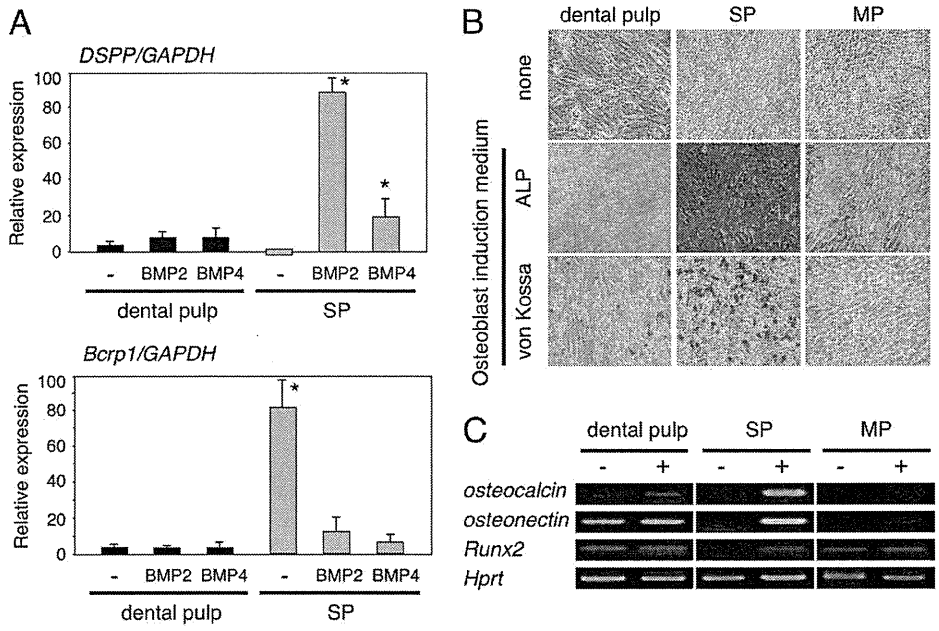

FIGURE 2. **Odontoblast and osteoblast differentiation in SP cells.** *A*, differentiation of SP cells to odontoblasts. Expression of the odontoblast marker DSPP and the undifferentiated mesenchymal marker Bcrp1 in dental pulp (*black bar*) and SP cells (*gray bar*) cultured with or without BMP2 or BMP4. *B*, differentiation of SP cells to osteoblasts in osteoblast induction medium (*Osteogenic cond.*). ALP and von Kossa staining of dental pulp, SP, and MP cells. *C*, expressions of osteoblast markers in dental pulp, SP, and MP cells cultured in regular (−) or osteoblast induction medium (+). *, $p < 0.05$.

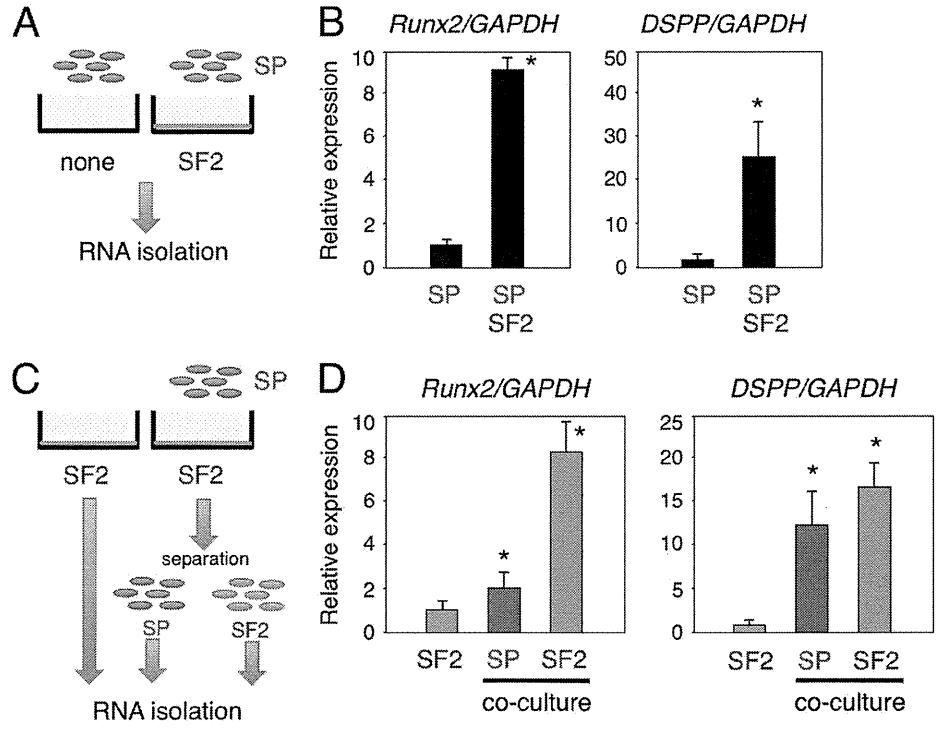

FIGURE 3. ***In vitro* epithelial-mesenchymal interaction system using dental epithelial cells (*SF2*) and dental mesenchymal stem cells (*SP*) to promote odontogenic cell differentiation.** *A* and *C*, schematic diagram of the co-culture system. *B*, comparisons of *Runx2* and *DSPP* gene expressions between the SP monolayer culture and SP and SF2 cell co-culture system. *C*, total RNA samples were separately prepared from SP and SF2 cells, using the anti-HA antibody. *D*, expressions of Runx2 and DSPP in co-cultured SF2 (*blue*) and SP (*red*) cells. The expression level of GAPDH was used an internal control. *, $p < 0.05$.

interaction produced by SF2 cells contributes to odontoblast induction. Denuded SF2 cells were also incapable of inducing DSPP expression in SP cells (Fig. 4*B*). Odontoblast induction of SP cells was observed in co-cultures with living SF2 cells, indicating that some types of soluble secreted molecules and matrices from SF2 cells are required to induce SP cells to undergo odontogenic differentiation.

Next, we screened the factors secreted from SF2 cells that promote odontogenic cell differentiation from epithelial and mesenchymal cells using cell culture chambers, which allowed

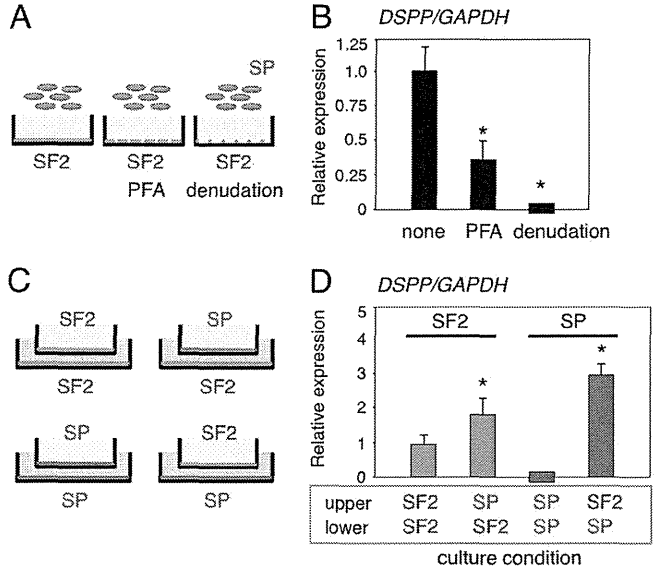

FIGURE 4. **Co-culture conditions for screening of odontogenic cell differentiation using *in vitro* cell-cell interaction system.** *A*, SP cells were cultured on SF2 cells in monolayers, then fixed with 4% paraformaldehyde (*PFA*) or treated with ammonia (denudation). *B*, DSPP expression in SP cells co-cultured under different conditions. *C*, four sets of co-culture conditions using cell chambers were analyzed. *D*, DSPP expression in SF2 cells (*blue*) and SP cells (*red*) cultured in lower dishes, with co-culture partner cells in the upper chambers. The expression level of GAPDH was used an internal control. *, $p < 0.05$.

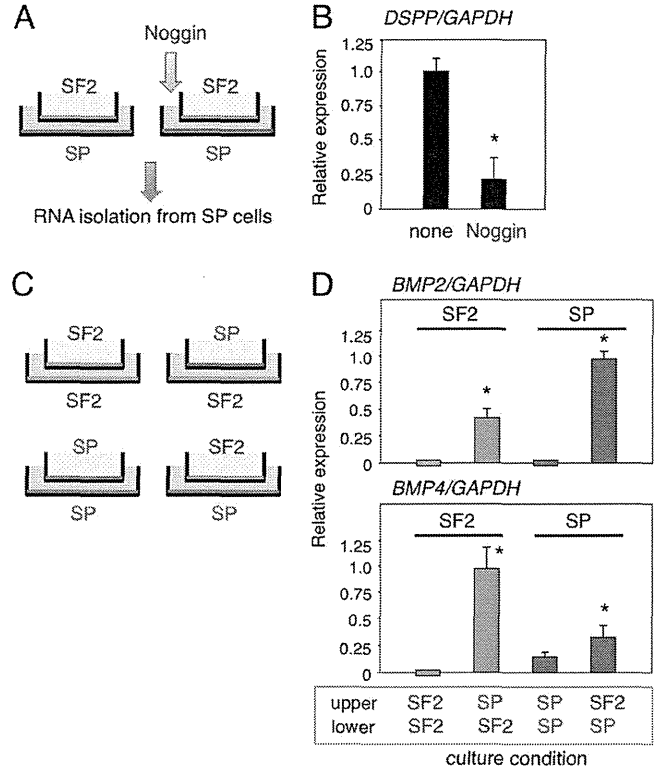

FIGURE 5. ***In vitro* epithelial-mesenchymal interaction system shows that crosstalk BMP signaling is essential for odontogenic cell differentiation.** *A*, total RNA was isolated from SP cells co-cultured with SF2 cells in the presence or absence of Noggin recombinant protein. *B*, DSPP expression in SP cells co-cultured with SF2 cells after blocking BMP signaling. *C*, four sets of culture conditions using cell chambers were analyzed. *D*, BMP2 and BMP4 expressions in SF2 (*blue*) and SP (*red*) cells, with co-culture partner cells in the upper chambers. *, $p < 0.05$.

the factors to be secreted into cell culture medium (Fig. 4*C*). Heterologous combinations of SF2 and SP cells were important for promotion of DSPP expression in both types of cells. We found that co-cultures consisting of SF2 cells in the upper chamber and SP cells in the lower chamber were most effective for stimulation of DSPP gene expression in SP cells (Fig. 4*D*). These results suggest that secreted factors are important for induction of DSPP expression in SP cells co-cultured with dental epithelial cells.

Regulation of DSPP Expression in SP Cells via BMP2-BMP4 Crosstalk—The involvement of several different types of growth factors has been reported in epithelial-mesenchymal interactions, for example, BMPs were shown to promote dental mesenchymal cell differentiation (27). We examined the potential involvement of BMPs in SP cell differentiation by adding soluble Noggin, which antagonizes BMP activity, to cell chamber cultures that contained SP cells in the lower chambers (Fig. 5*A*). The presence of Noggin in culture medium resulted in down-regulation of the expression of DSPP in SP cells as compared with the control cells (Fig. 5*B*). Therefore, BMPs are required for induction of DSPP expression in SP cells co-cultured with dental epithelial cells. In tooth germ development, BMP4 is involved in epithelial-mesenchymal interaction, and also regulates the mesenchymal expression of Msx1 and Msx2, which are important for tooth development, whereas BMP2 promotes dental mesenchymal differentiation (27). However, details regarding crosstalk between BMP2 and BMP4 in dental epithelial and mesenchymal stem cell interactions have not been elucidated. We sought to clarify the role of BMPs in these interactions by examining the expressions of BMP2 and BMP4 in SF2 and SP cells using a separated chamber assay (Fig. 5*C*). The expression of BMP2 was higher in SP cells than SF2 cells under the heterologous combination culture condition, whereas BMP2 was not detected in homologous cultures (Fig. 5*D*). In contrast, the expression of BMP4 was higher in SF2 cells than in SP cells in the heterologous combinations (Fig. 5*D*). Taken together, these results suggest that the interactions between dental epithelium and dental mesenchymal stem cells induce BMP4 and BMP2, which, in turn, promote odontogenic cell differentiation via paracrine and autocrine signaling.

Optimization of Co-culture Conditions for Differentiation of iPS Cells into Ambn-expressing Dental Epithelial Cells—Following interaction with SF2 cells, SP cells differentiated into DSPP expressing cells, but not ameloblasts (Figs. 3, 4, and 5). This may be because SP cells are mesenchymal stem cells and committed to differentiate into mesenchyme lineage cell types. Therefore, we used mouse iPS cells to examine whether these cells can be differentiated into ameloblasts when cultured with SF2 cells. However, SF2 cells did not effectively promote their differentiation (data not shown), which may be due to the necessity of factors from differentiated dental epithelial cells for differentiation of iPS cells into ameloblasts. To test this possibility, we subcloned 25 different SF2 cell lines and examined the expression levels of the Ambn gene. Of these lines, the SF2-24 cell line expressed Ambn at the highest level (supplemental Fig. S3*A*). Dental epithelium SF2-24 cells grew tightly together in a

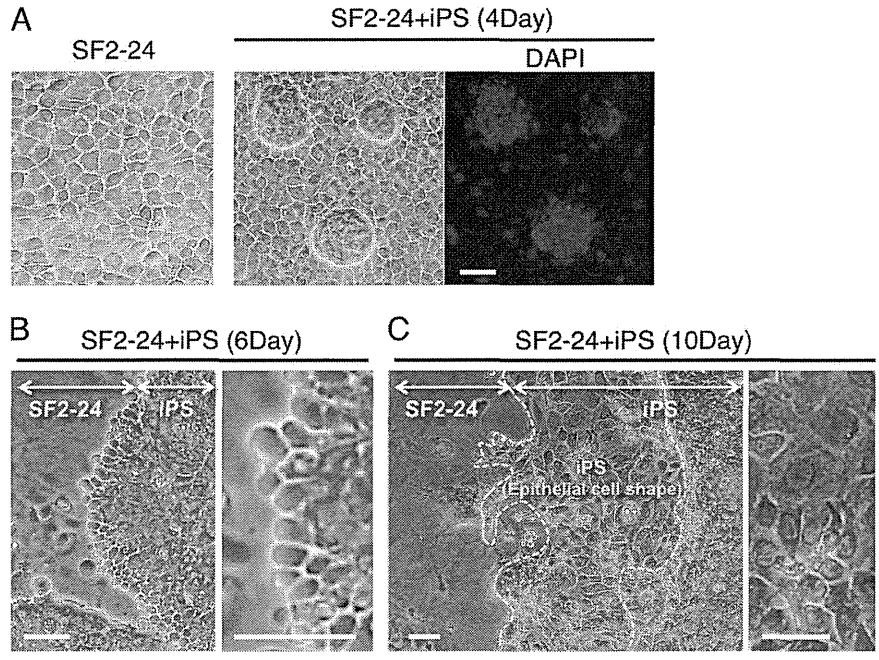

FIGURE 6. **Epithelial cell shapes of iPS cells after co-culturing with SF2-24 cells.** *A*, phase micrographs of monolayer SF2-24 cells and iPS cells cultured with SF2-24 feeder cells for 4 days, followed by DAPI staining. *B* and *C*, low and high magnification phase micrographs of iPS cells on MMC-treated SF2-24 feeder cells after 6 (*6Day*) and 10 days (*10Day*). Enlarged image shows a part of the iPS cells with epithelial cell shapes. *C*, epithelial cell cluster formed by iPS cell-derived epithelial cells (area within *yellow dashed line*). Bar, 50 mm.

square or cuboidal shape (Fig. 6*A*), and expressed Ambn and cytokeratin-14 (CK14), but not the reprogrammed factors Sox2, Klf4, and Oct3/4 (supplemental Fig. S3*B*). On the other hand, iPS cells formed colonies that expressed Nanog promoter-driven GFP (data not shown) as well as Klf4, Sox2, Oct3/4, and Nanog, but not Ambn or CK14 (supplemental Fig. S3*B*).

We also examined the effects of differentiation by co-culturing iPS cells with MMC-treated non-proliferating SF2-24 feeder cells (Fig. 6*A*). The shape of the co-cultured iPS cells was clearly rounded along the boundary of the clusters after 6 days (Fig. 6*B*). These cells had migrated and formed what appeared to be epithelium after 10 days (area surrounded by *yellow dashed line*, Fig. 6*C*).

The differentiation of iPS cells was then determined by RT-PCR analysis. First, we examined the specificity of mouse Ambn locked nucleic acid (LNA) primer sets (supplemental Fig. S4). A mouse Ambn LNA primer set specifically detected the mouse Ambn gene, but not the rat Ambn gene (supplemental Fig. S4*A*). Using this primer set, Ambn expression was not detected in mouse iPS cells or MEFs (supplemental Fig. S4*B*). Next, we examined co-culture conditions for the differentiation of iPS cells into dental epithelium (Fig. 7*A*). iPS cells co-cultured with MMC-treated SF2-24 cells showed a high expression of the mouse Ambn gene, while those co-cultured with PFA-treated or non-treated SF2-24 cells did not (Fig. 7*B*). SF2-24 feeder cells expressed rat Ambn when co-cultured with iPS cells, while that expression was reduced at 10 days (Fig. 7*C*).

Interestingly, expressions of the stem cell markers Sox2, Oct3/4, Nanog, Fgf4, and Gdf3 were not changed throughout the co-culture period, because of the existence of undifferentiated iPS cells (Fig. 7*C*), while those of the endodermal markers Cdx2 and Gata6 were also not increased. Furthermore, the mesodermal marker Brachyury was highly expressed in iPS cells, because of technical contamination resulting RNA extraction from MEFs used for maintenance of the iPS cells, and then gradually decreased over time. We also observed increased expressions of the mouse ameloblast markers Ambn and Enamelin (Enam), as well as the epithelial markers CK14 and p63, in iPS cells after 7 and 10 days (Fig. 7*C*). Furthermore, the expression of epiprofin/Sp6, a transcription factor highly expressed in dental epithelium (28), was increased in those cells (supplemental Fig. S5). A similar expression pattern was observed in co-cultured iPS cells separated from SF2-24 cells using the anti-HA antibody (data not shown).

Differentiation of iPS Cells into Ambn-expressing Dental Epithelial Cells—We then examined the protein expression of Ambn in iPS cells using immunostaining. Approximately 95% of the epithelial-like cells were positive for Ambn (Fig. 8*A*), while the immunofluorescence intensity of Ambn was stronger in iPS cells than in SF2-24 cells (Fig. 8*B*). Therefore, mouse iPS cells differentiated into dental epithelium, but not into endodermal or mesodermal cells.

We attempted to identify the factors involved in differentiation of iPS cells into dental epithelium by culturing with MEFs in medium conditioned by SF2-24 cell cultures (Fig. 9*A*). Culturing with SF2-24 condition medium induced the expression of Ambn in iPS cells, indicating an involvement of soluble factors including growth factors, and extracellular matrices derived from SF2-24 cells (Fig. 9*B*). Next, we examined the effect of Ambn on differentiation of iPS cells into dental epithelial cells. Expression vectors for the full-length (AB1), C-terminal (AB2), and N-terminal (AB3) half of Ambn (Fig. 9*C*) were separately transfected into Ambn low-expressing cells (SF2-7), then conditioned media from those cells or recombinant Ambn

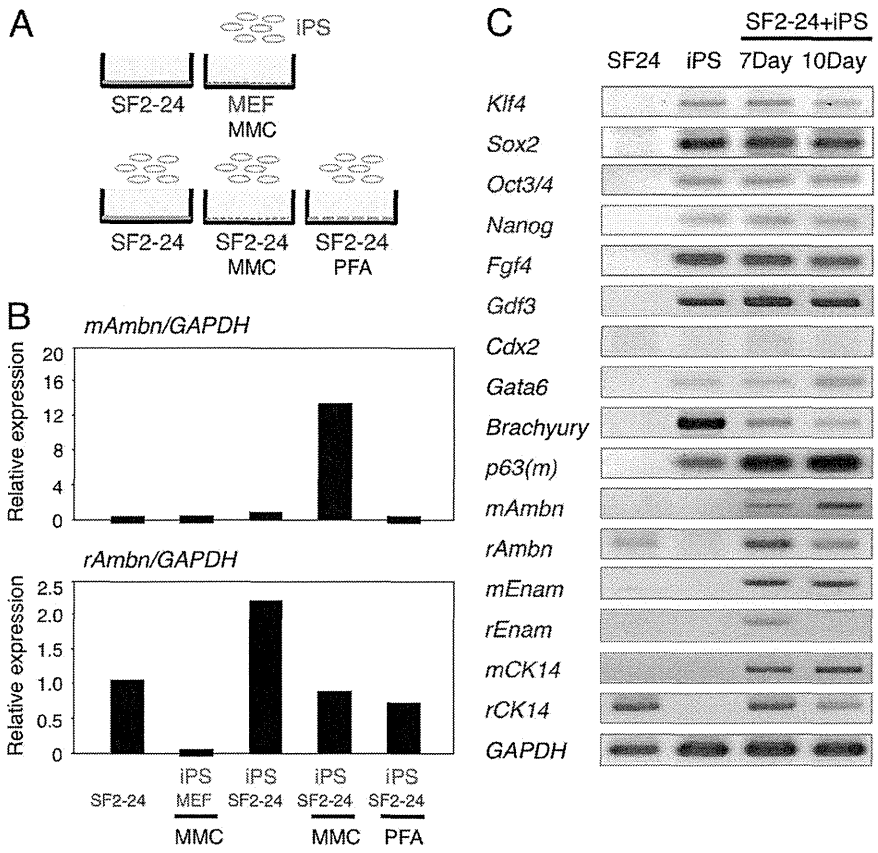

FIGURE 7. **Effects of culture conditions on ameloblast induction of iPS cells.** *A*, iPS cells were co-cultured with SF2-24 cells, MMC-treated (*MMC*) MEFs, MMC-treated SF2-24 cells or PFA-treated SF2-24 cells. *B*, Ambn expression in mouse iPS (*upper panel*) and rat-derived SF2-24 (*bottom panel*) cells in different co-culture conditions for 10 days. *C*, time course analysis of gene expressions of stem cell (*blue*), endo/mesoderm (*black*), and ameloblast (*red*) markers in iPS cells co-cultured with SF2-24 cells for 7 (*7Day*) and 10 days (*10Day*).

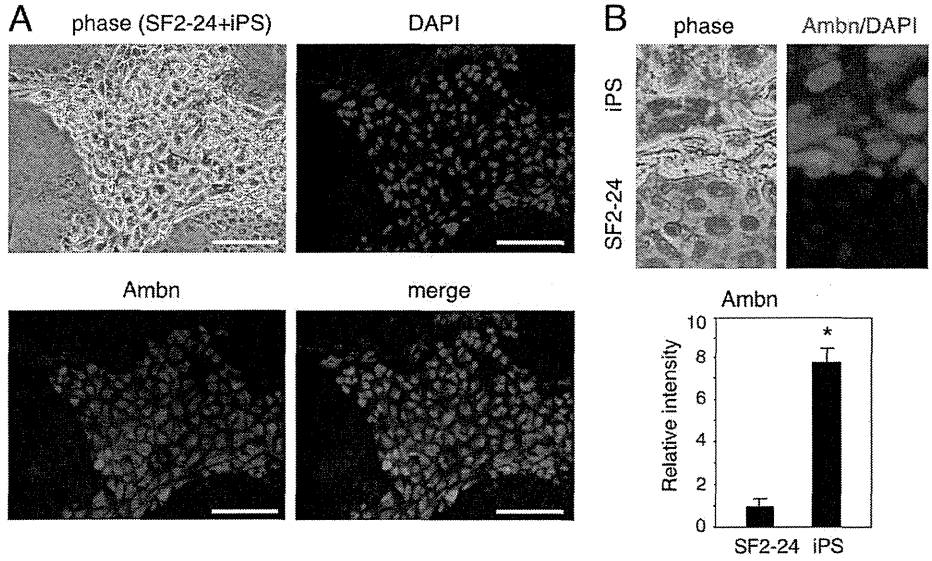

FIGURE 8. **Expression of Ambn, an ameloblast specific protein, in iPS cells co-cultured with SF2-24 cells.** *A*, phase micrographs of iPS cell colonies cultured with mitomycin C-treated SF2-24 cells. Hoechst staining (*blue*), Ambn staining (*red*), and merged images. *B*, high magnifications of phase and merged images in *A*. *Bottom panel*, relative expression levels of Ambn protein in SF2-24 and iPS cells cultured in ameloblast induction system. *, $p < 0.05$; Bar, 100 mm.

proteins (AB1, -2, or -3) were added to cultures of iPS cells. Conditioned media from SF2-24 cells and full-length AMBN-expressing cells, but not from other transfectants or recombinant Ambn proteins, induced Ambn expression in iPS cells (Fig. 9*D*), indicating that Ambn may be necessary for differentiation of iPS cells into dental epithelium. Previously, we showed that neurotrophic factor NT-4 is important for the differentiation of ameloblasts (29). To examine the effect of NT-4